

EVALUATION OF SUBSURFACE FLOW IN FISSURED SEDIMENTS
IN THE CHIHUAHUAN DESERT, TEXAS

Final Report

prepared by

Bridget R. Scanlon and Richard S. Goldsmith

Bureau of Economic Geology
Noel Tyler, Director
The University of Texas at Austin
Austin, Texas 78713-8924

for

National Low-Level Radioactive Waste Management Program,
U.S. Department of Energy,
Assistant Secretary for Environmental Management,
under DOE Idaho Operations Office Contract No. DE-AC07-95ID 13223 and
Interagency Contract No. 94-0304

June 1995

CONTENTS

Abstract	1
Introduction	2
Previous Studies	3
Objectives	4
Soil Physics	4
Electromagnetic Induction	5
Environmental Tracers	5
Site Description	6
Methods	8
Results	11
Texture and Water Content	11
Soil Water Potential	12
Plant Water Potential	13
Environmental Tracers	14
Meteoric Chloride	14
Isotopes	15
Electromagnetic Induction	16
Discussion	18
Subsurface Water Movement in Fissured Sediments	18
Water Flux Estimates	19
Piston versus Preferential Flow	21
Evaluation of Different Techniques to Estimate Flow in Fissured Sediments	22
Conclusions	24
Acknowledgments	25
References	25

Figures

1. Map of fissures in study area
2. Profiles of texture, gravimetric water content, water potential, and chloride concentrations in and adjacent to Hueco Bolson and Eagle Flat fissures
3. Profiles of texture, gravimetric water content, water potential, and chloride concentrations in and adjacent to Red Light Bolson and Ryan Flat fissures
4. Variation in water content with depth and time in neutron probe access tubes in and 10 m distant from Eagle Flat fissure
5. Predawn plant water potentials measured in and adjacent to fissures
6. Variations in ^3H and $^{36}\text{Cl}/\text{Cl}$ in profiles in and adjacent to fissures
7. Stable isotopes of oxygen and hydrogen for a profile beneath Red Light Bolson fissure and 50 m distant from the fissure
8. Electromagnetic transects across fissures

Tables

1. Texture and gravimetric water content of soil samples collected beneath and adjacent to fissures
2. Gravitational, water, total, and osmotic potentials of soil samples collected beneath and adjacent to fissures
3. Gravimetric water content, chloride concentrations, water flux, water velocity, age, cumulative chloride, and cumulative water content of soil samples
4. Tritium and $^{36}\text{Cl}/\text{Cl}$ ratios and stable isotopes of oxygen and hydrogen in samples collected beneath and adjacent to fissures

EVALUATION OF SUBSURFACE FLOW IN FISSURED SEDIMENTS IN THE CHIHUAHUAN DESERT, TEXAS

ABSTRACT

Fissures are surface features, or gullies, some of which are underlain by sediment-filled fractures. A previous study of subsurface flow beneath a fissure showed higher water fluxes beneath the fissure, which was attributed to infiltration of ponded water in the fissure. This study was conducted to investigate the vertical and lateral extent of increased flow associated with fissured sediments, to compare subsurface flow beneath fissures of different maturity, and to examine different techniques for evaluating flow in fissured zones. Boreholes were drilled directly beneath four fissures and at distances of 10 m and 50 m from the fissures, and soil samples were analyzed for various soil physics parameters and environmental tracer distribution. Electromagnetic induction was used to map apparent conductivity in transects perpendicular to the fissures.

Fissures had higher water potentials and lower chloride concentration than surrounding sediments. Zones of high flux were restricted to the area directly beneath some fissures, whereas others also had high fluxes in the profiles 10 m distant from the fissure. Water potential and chloride fronts were found beneath two of the fissures in the upper 20-m zone, which indicates that most of the flow occurred in this zone. Water flux estimates, based on the position of the chloride front and an assumed age of the fissures of 50 yr, ranged from 28 to 48 mm yr⁻¹. High tritium levels were found throughout the fissured profiles (to maximum depth of 26.4 m) and in some cases in the profiles 10 m distant from the fissure, indicating post-1952 water. The occurrence of high tritium levels beneath the chloride front in one fissure indicates that some of the water is flowing preferentially. Minimum estimates of water flux based on the tritium data ranged from 28 to 120 mm yr⁻¹. Stable isotopes of oxygen and hydrogen were less enriched beneath the fissure, which is consistent with higher fluxes beneath the fissure. Plant water potentials were of limited

use in delineating fissure flow. Apparent conductivities were higher across two fissures, whereas the other two fissures did not show any variation in apparent conductivity. The higher conductivity in some fissures is attributed to higher water content. Multiple independent lines of evidence indicate that subsurface water fluxes are higher beneath fissures.

Variations in measured parameters were found among fissures and were attributed to the different stages of maturity of the fissures examined. As fissures mature, they are filled with sediment and no longer actively concentrate surface runoff and therefore should dry out. Multiple profiles drilled in one fissure indicate that there can be large variability in flow along fissures.

INTRODUCTION

Surface fissures have been found in semiarid and arid regions throughout the western United States from southern California to western Texas and as far north as Idaho (Baumgardner and Scanlon, 1992). Linear systems of fissures may be as much as 15 km long (Slaff, 1989). Individual fissures as wide as 15 m and fractures as deep as 25 m have been found (Boling, 1986; Slaff, 1989).

The term *fissure* refers to the alignment of discontinuous surface collapse structures, or gullies; the underlying extensional feature, termed a *fracture*, is filled with sediment. Fissures commonly form in unconsolidated sediments near margins of alluvial valleys. They are generally oriented parallel or subparallel to the long axis of the host valley and approximately perpendicular to tributary drainage. Because of their orientation they intercept runoff, which erodes the fissures into wide gullies. The increased runoff in fissured sediments results in vegetation being concentrated in these zones.

Many fissures have formed where land subsidence has resulted from groundwater withdrawal, particularly in Arizona (Schumann and others, 1986). However, some fissures have formed in areas where groundwater pumping has been minimal or before extensive groundwater pumping began (Slaff, 1989; Robinson and Peterson, 1962). Baumgardner and Scanlon (1992) suggested that the model for fissure development proposed by Larson and Péwé (1986) should be

applicable to fissures in the study area. According to this model, the initial feature is a fracture that forms in the shallow subsurface and allows water to move down from the surface. Water movement leads to erosion of the fracture and creates a soil pipe. Eventually the sediments overlying the pipe collapse into the cavity, which results in surface gullies that concentrate runoff; the gullies eventually connect, and the final phase is marked by plugging of the soil pipe at the outlet and filling of the fissure with sediment.

Previous Studies

Geomorphic and hydrologic studies conducted in the Hueco Bolson fissure are described in Baumgardner and Scanlon (1992) and Scanlon (1992b). Soil physics and environmental and applied tracer studies were conducted to evaluate subsurface flow in the fissured sediments. Collection of soil samples was restricted to a profile beneath the fissure and two profiles at distances of 3 m and 6 m from the fissure. The maximum borehole depth was 9.3 m. These samples were analyzed for texture, water content, water potential, and chloride concentration. In addition, a tracer experiment was conducted in a trench dug to 4 m depth to evaluate flow and transport in the fracture fill relative to the surrounding sediments. The results of these studies showed that subsurface water fluxes were higher beneath the fissure, as indicated by higher water potentials and lower maximum chloride concentrations (80 to 105 g m⁻³), than those in surrounding geomorphic settings (Cl concentrations; 2000 to 6000 g m⁻³). The applied tracer experiment showed higher water and solute transport in the fracture fill sediment than in adjacent sediments. The fissure was marked by a lineation of dense stands of *Prosopis glandulosa* (Honey mesquite), and roots of these plants extended to at least 6 m in the fracture-fill sediments, which suggests that plants may play an important part in removing water from these areas.

Objectives

The objectives of this study were to compare subsurface flow beneath fissures of different maturity, to determine the vertical and lateral extent of subsurface flow in fissured sediments, and to evaluate different techniques of estimating subsurface flow. Additional studies were conducted in the Hueco Bolson fissure, and three new fissures were examined to evaluate variations in subsurface water movement among fissures of different age, as indicated by width-to-depth ratios of surface gullies associated with the fissures. The vertical extent of subsurface flow was evaluated by drilling and sampling boreholes to a maximum depth of 31 m, whereas in the previous investigation the maximum borehole depth was 9.3 m. To evaluate the lateral extent of increased flow associated with fissures, boreholes were drilled at distances of 10 and 50 m from each fissure; the previous study only included boreholes at distances of 3 and 6 m. Previous studies used soil physics and environmental tracer techniques to evaluate flow in fissured sediments (Baumgardner and Scanlon, 1992). In this study we also investigated noninvasive techniques such as electromagnetic induction and measurement of plant water potentials. The following provides a brief description of the theoretical basis for the various techniques used.

Soil Physics

Soil physics data included measurement of water content and water potential on soil samples collected from boreholes drilled in and adjacent to the fissures. Water content is discontinuous across different soil types; therefore, variations in water content measured at one time cannot be used to evaluate the direction of water movement. In contrast, water potential is continuous across different soil types and water potential gradients can be used to assess the direction of water movement. Predawn plant water potentials are generally considered to give an indication of the soil water potential and to provide a noninvasive technique of estimating subsurface flow. Because vegetation, particularly mesquite, is much more dense along fissures than in adjacent nonfissured sediments, vegetation probably plays an important role in controlling

subsurface water movement. Previous studies showed that soil water potentials were much higher in fissured sediments than in adjacent nonfissured sediments; therefore, predawn plant water potentials in fissured zones should be higher than in adjacent nonfissured sediments.

Electromagnetic Induction

Electromagnetic induction was used to evaluate subsurface flow in fissured sediments. Electromagnetic induction provides a noninvasive technique of evaluating apparent conductivity of the soil. Fractures and soil pipes with associated high water flux may exist in the subsurface for a long time with little surface expression; therefore, noninvasive techniques may be particularly useful for delineating these zones prior to surface collapse and gully formation. Previous studies of fissured sediments showed that soil water chloride was flushed out in fissured sediments. Zones of low soil water chloride concentration are particularly characteristic of fissured sediments, and it was thought that they should result in low apparent conductivity that could be detected with electromagnetic induction.

Environmental Tracers

Environmental tracers are being used extensively to quantify subsurface water fluxes. Chloride concentrations in soil water have been widely used to evaluate water fluxes in arid and semiarid systems (Allison and Hughes, 1978; Edmunds and Walton, 1980). Chloride concentrations in soil water increase through the root zone as a result of evapotranspiration because chloride is essentially nonvolatile and plant uptake is negligible. The net downward water flux can be estimated by dividing the chloride deposition rate by the chloride concentration in soil water. The residence time represented by chloride at depth z can be evaluated by dividing the cumulative total mass of chloride from the surface to that depth by the annual chloride deposition

$$t = \frac{\int_0^z \theta C_{Cl} dz}{D_{Cl}} \quad (1)$$

where θ is the volumetric water content, C_{Cl} is the chloride concentration of soil water, and D_{Cl} is the chloride deposition rate. The above technique is known as the chloride mass balance technique and assumes one-dimensional, vertical, downward, piston-type flow; precipitation as the only source of chloride; annual chloride deposition constant with time; and a steady-state water flux. These assumptions need to be evaluated when this technique is used. In some areas it is not possible to quantify the rate of water movement on the basis of chloride concentrations in soil water, and in these cases the presence or absence of chloride can be used as a qualitative indicator of the rate of subsurface water flow. Low chloride concentrations reflect high water fluxes, which either minimize accumulation of chloride or flush out previously accumulated chloride.

The subsurface distribution of bomb pulse tracers such as chlorine-36 and tritium provides information on water movement during the past 30 to 40 yr. Chlorine-36 (half-life $301\,000 \pm 4000$ yr) was enriched by neutron activation of chlorine-35 in sea water by weapons tests that were conducted between 1952 and 1958 and peaked in 1955 (Bentley and others, 1986). Chlorine-36 production as a result of weapons testing exceeded natural production by up to three orders of magnitude (Bentley and others, 1986). Chlorine-36 is a tracer of liquid flow because chlorine-36 entered the hydrologic cycle as chloride, which is essentially nonvolatile. Tritium (half-life 12.43 ± 0.05 yr) concentrations increased from 10 to ≥ 2000 TU during atmospheric nuclear testing that was initiated in 1952 and peaked between 1963 and 1964. Tritiated water can exist in both liquid and vapor phases; therefore, tritium is a tracer for liquid and vapor water movement.

Site Description

Fissures examined in this study are located in intermontane basins within the Basin and Range physiographic province in Trans-Pecos Texas (fig. 1). Additional studies were conducted in the Hueco Bolson fissure, and three other fissures were included in this investigation. All fissures are found in alluvial fill sediments. Depth to groundwater ranges from 85 m (Ryan Flat fissure) to 215 m (Eagle Flat fissure).

Three of the four fissures studied are described in detail in Baumgardner and Scanlon (1992), and the fourth fissure (Eagle Flat) is described in Jackson and others (1993); therefore, only brief descriptions are provided here. The names of some of the fissures have been changed; i.e., Hoover fissure in Jackson and others (1993) corresponds to Eagle Flat fissure, and Quitman Canyon fissure in Baumgardner and Scanlon (1992) is now called Red Light Bolson fissure. Width-to-depth ratios of fissures, which provide some indication of the stability and age of the fissures, range from 0.1 to 28; however, most are ≤ 5 . Fissures with very low width-to-depth ratios are unstable and are still undergoing collapse, whereas those with high width-to-depth ratios are probably filling and widening.

Three fissures were mapped in the Hueco Bolson and ranged from 21 to 140 m long. These fissures are in the Camp Rice Formation, which consists of fairly coarse textured sediments. Studies were conducted in the 140-m-long fissure, which had width-to-depth ratios that ranged from 0.2 to 2. This fissure is marked by dense growth of mesquite trees (*Prosopis glandulosa*). The surface collapse features are separated by bridges of sediment that overlie soil pipes. Spacing between collapsed sections is generally 1 to 3 m. Trenches revealed subsurface fractures that extend to a depth of at least 6.2 m. The fracture ranges from 65 mm at 3.8 m depth to 25 mm at 5.6 m depth and is filled with sediment. The fissure is not visible on aerial photographs because of large creosote bushes (*Larrea tridentata*) adjacent to the fissured sediments.

The fissure studied in Red Light Basin lies at the toe of a dissected alluvial fan. The fissure trends N10° - 25°W, parallel to topographic contours and to the valley axis. These fissures were up to 4.2 km long on aerial photographs taken in 1957. The northwest-trending fissures are perpendicular to the ephemeral stream channels and intercept runoff. Mesquite trees are denser in the vicinity of the fissure. These fissures have filled with sediment and have width-to-depth ratios up to 5. Another section of the Red Light Bolson fissures showed evidence of recent collapse and had steep gullies (3.55 m deep and 0.75 m wide).

The Eagle Flat fissure examined in this study is described in Jackson and others (1993) and differs in location from Eagle Flat fissures described in Baumgardner and Scanlon (1992), which

are located in the Booth property. This fissure is 1.2 km long and is clearly delineated by vegetation on aerial photographs and on the ground. It consists of depressions that average 20 m long, 1 m wide, and 0.3 m deep. The large width-to-depth ratio indicates that the fissure is old. Trenches indicate that there is no well-defined fracture beneath the fissure. There is a gap in the uppermost calcic horizon beneath the fissure that may have resulted from blocks of material falling into the fissure or from dissolution and reprecipitation of calcic material.

Fissures in Ryan Flat formed in 1990. This fissure was 2.2 m deep and 0.7 m wide at its deepest part, which results in a width-to-depth ratio of 0.1 and is consistent with the young age of the fissure. Traces of an old fissure near the 1990 fissure are indicated by elongate shallow swales and aligned mesquite bushes adjacent and parallel to the new fissure. This suggests that the new fissure is opening where an older fissure existed. Surface collapse of sediment was reported in 1935 also and probably marks the timing of the original fissure.

METHODS

Soil samples were collected for laboratory measurement of particle size, gravimetric water content, and chloride concentration from 14 boreholes drilled in and adjacent to four fissures (fig. 1). Selected samples from different profiles were analyzed for tritium and chlorine-36. Borehole depths ranged from 8.7 m (RLB 50m) to 30.6 m (EFF36 10m).

Particle size analyses were conducted on selected soil samples from different profiles where large variations in water content were found (table 1). Carbonate was not dissolved in these samples because some of the rock fragments were carbonate. The ≥ 2 -mm fraction was determined by sieve analysis, and the percent silt and clay were determined by hydrometer analysis (Gee and Bauder, 1986). Sediment samples that contained $\geq 3\%$ gravel were classified according to Folk (1974), and those that lacked gravel were classified according to the U.S. Department of Agriculture (1975). Gravimetric water content was measured by oven drying the soil samples at 105°C for 24 hr. To determine chloride content, double-deionized water was added to the dried soil sample in a 3:1 ratio. Samples were agitated on a reciprocal shaker table for 4 hr. The supernatant

was filtered through 0.45- μm filters. Chloride was then analyzed by ion chromatography or by potentiometric titration.

Laboratory preparation of chloride samples for chlorine-36 analysis followed procedures outlined in Scanlon (1992a). The $^{36}\text{Cl}/\text{Cl}$ ratios were measured by tandem accelerator mass spectrometry (TAMS) at Lawrence Livermore National Laboratory. To evaluate chemical contamination during sample preparation, reagent-grade NaCl was subjected to the same purification procedure as the soil samples. Uncertainties were calculated following Elmore and others (1984) and are reported as one standard deviation.

Water for tritium analysis was extracted from soil samples by azeotropic distillation with toluene (Allison and others, 1985). After distillation the water samples were purified of toluene by heating in paraffin wax. Tritium was analyzed by the University of Arizona Tritium Laboratory using an enrichment factor of 8 for samples of ≥ 150 mL and slightly less for smaller samples. The detection limit for enriched tritium analyses was 0.7 TU, and the standard errors were ≤ 1.3 TU. Water for analysis of stable isotopes of oxygen and hydrogen was extracted by distillation with toluene (Ingraham and Shadel, 1992) by Desert Research Institute.

Water potential was measured in the laboratory using a thermocouple psychrometer with a sample changer (model SC-10) manufactured by Decagon Devices, Inc., Pullman, WA. The Decagon SC-10 was calibrated using NaCl solutions that ranged in concentration from 0.05 M to saturated and corresponded to water potentials of -0.2 to -38 MPa at 20°C (Lang, 1967). The standard error of estimate for the SC-10 thermocouple psychrometer, based on analysis of 20 calibration solutions, was 0.06 MPa. The osmotic component of water potential was calculated according to the van't Hoff equation (Campbell, 1985; Scanlon, 1994).

Neutron probe access tubes were installed beneath Eagle Flat fissure and 10 m distant from the fissure to a depth of 8.5 m to monitor temporal variations in water content. Water content was monitored with a Campbell Pacific Nuclear neutron moisture probe (Model 503DR; CPN Corporation, Martinez, CA).

Predawn plant water potentials were obtained using a portable pressure chamber apparatus (Plant Moisture Stress, Inc., Corvallis, OR) by removing ≥ 2 randomly chosen stems containing leaves from each plant and immediately measuring their water potential. The stems were wrapped in plastic to minimize sample drying prior to measurement and to prevent sample burning by nitrogen in the pressure chamber. Stems were collected from mesquite plants within and adjacent to each fissure except in the area adjacent to the Hueco Bolson fissure, where mesquite trees were not found. Creosote bushes were found in and adjacent to the Hueco Bolson fissure, and these were sampled for water potential. Water potential measurements were conducted from October 1994 through May 1995. Samples were not collected in March because the plants defoliated and were dormant.

Geonics instruments were used to measure apparent conductivity of the soil along transects perpendicular to the fissures. The theoretical basis for these measurements is described in McNeill (1992). These instruments consist of a transmitter coil placed on the ground that is energized with an alternating current at an audio frequency. This current generates a primary magnetic field, which in turn induces small currents that generate their own secondary magnetic field. The receiver coil responds to both the primary and secondary magnetic field components. Under low values of induction number, the secondary magnetic field is a linear function of conductivity. Two instruments were used in this study, the EM38 and the EM31. The intercoil spacing in the EM38 is 1.0 m, whereas that in the EM31 is 3.7 m. The difference in intercoil spacings results in different exploration depths for these instruments: 0.75 m for the EM38 and 3.0 m for the EM31 when the instrument is operated in the horizontal dipole mode (both coils lying vertically on the ground) and 1.5 m for the EM38 and 6 m for the EM31 when the instrument is operated in the vertical dipole mode (both coils lying horizontally on ground). Both instruments were operated in the horizontal and vertical dipole modes in this study to evaluate changes in conductivity with depth. EM transects were conducted perpendicular to each of the fissures, generally for a distance of 100 m on either side of the fissure.

RESULTS

Texture and Water Content

Soil texture was variable among fissures (table 1). Soil texture in and adjacent to the Hueco Bolson and Red Light Bolson fissures is much coarser grained than that in and adjacent to Eagle Flat and Ryan Flat fissures. Sediment samples beneath and adjacent to the Hueco Bolson fissure range from 48% clay (HBF 0m) to 80% gravel (HBF 50m). Textures in the Red Light Bolson fissure are predominantly muddy sandy gravel (gravel 32 to 65%). In contrast, textures beneath Eagle Flat fissure range from clay to muddy sandy gravel and those beneath Ryan Flat fissure are predominantly clay, with local zones of gravelly material ($\leq 41\%$ gravel). Profiles 10 m distant from Eagle Flat fissure were finer grained (predominantly clay) than those beneath the fissure (predominantly loam). In the case of all the other fissures, there were no systematic differences in texture between the profiles in the fissure relative to those adjacent to the fissure.

The relationship between water content beneath and adjacent to the fissures was variable (figs. 2 and 3). Laboratory-measured water content was higher beneath Eagle Flat fissure than in the profiles 10 m distant from the fissure (table 1; fig. 2d, g, and j). Correlations between water content and texture were high, particularly for the profiles beneath the fissure. Water content was negatively correlated with percent sand and positively correlated with percent clay (table 1). Higher water contents beneath Eagle Flat fissure cannot be attributed to textural differences in profiles beneath and adjacent to the fissure because of the sandier soil beneath the fissure and the negative correlations between sand and water content. The higher water contents beneath Eagle Flat fissure reflect higher water fluxes in this zone, as seen in water-content changes monitored down to 1.5 m in the neutron probe access tube installed in Eagle Flat fissure; water content monitored in the neutron probe access tube 10 m distant from the fissure was temporally invariant (fig. 4). The remaining fissures did not show any systematic variation in water content beneath the fissure relative to water content adjacent to the fissure. Water contents beneath Ryan Flat fissure were similar to those in adjacent profiles in the upper 3 m but were generally higher beneath the fissure

at greater depths (fig. 3d); however, these water-content differences at depth can be explained by textural variations. Correlations between water content and texture were high (table 1). Profiles beneath Red Light Bolson (fig. 3a) and Hueco Bolson (fig. 2a) fissures displayed no systematic variation in water content relative to adjacent profiles. Spatial variability in water content in these profiles is related to textural variations; negative correlations with percent gravel and/or sand and positive correlations with percent clay (table 1).

Soil Water Potential

Soil water potentials (sum of matric and osmotic potential) were generally higher in profiles beneath the fissures than in profiles adjacent to the fissures in the upper 6 to 15 m (figs. 2 and 3; table 2). Water potentials were as high as -0.3 MPa beneath the Hueco Bolson, Eagle Flat, and Ryan Flat fissures. The values of these water potentials may not be highly accurate because of the standard error of the laboratory-measured water potentials in this range (~ 0.02 MPa). Some of the profiles in the fissures have a zone of low water potentials in the surficial sediments that reflects evaporation (figs. 2b, h, k, and 3e). The Eagle Flat fissure differs from the other fissures in that soil water potentials decrease below the zone of high water potentials, whereas in all the other profiles water potentials remain high at depth. This reduction in water potential at depth in the Eagle Flat fissures marks the wetting front and is most clearly seen in EFF35 0m (fig. 2e); the wetting front is more diffuse in the other two profiles beneath Eagle Flat fissure (fig. 2h and k). In profile EFF35 0m, water potentials decrease from -0.8 MPa at 9.1 m to -5.0 MPa at 12.8 m depth. Below 13 m, water potentials in EFF35 0m are similar to those in the profile 10 m distant from the fissure EFF36 10m. Water potentials in the other two profiles beneath Eagle Flat fissure (EFF88 0m and EFF92 0m) were generally lower than those in EFF35 0m.

The equilibrium line plotted on all graphs (figs. 2 and 3) represents that matric potential that would exist if the unsaturated zone were in equilibrium with the water table. This line represents a no-flow line where matric and gravity forces are balanced. Matric potentials that plot to the right of the equilibrium line indicate downward flow, whereas matric potentials that plot to the left of the

equilibrium line indicate upward flow under steady flow conditions. The osmotic component of water potential was negligible beneath the fissures because of low chloride concentrations (table 2). The zone of high water potentials beneath the fissures plots to the right of the equilibrium line, indicating downward flow. The exception is water potentials in Red Light Bolson fissure, which plot to the left of the equilibrium line (fig. 3b). The zone of low water potentials in the shallow subsurface in some profiles beneath the fissure also plot to the left of the equilibrium line, indicating evapotranspiration.

Water potentials in profiles adjacent to the fissures were low at the surface (≥ -27.4 MPa) and generally increased with depth, which indicates an upward driving force for water movement. These profiles also plot to the left of the equilibrium, which further indicates upward flow.

Plant Water Potential

Predawn plant water potentials were significantly ($\alpha=0.05$) higher in Hueco Bolson and Ryan Flat fissures than adjacent to these fissures (fig. 5). In contrast, there was no systematic difference in predawn plant water potentials between Eagle Flat and Red Light Bolson fissures. The difference in predawn plant water potentials was most obvious in Ryan Flat fissure (fig. 5c), which is a very active fissure. The average plant water potential in this fissure ranged from -1.43 to -1.98 , whereas that in plants adjacent to the fissure ranged from -3.25 to -4.4 . Seasonal variations in predawn plant water potential were low. Measurements in January showed large variability in plant water potentials adjacent to the fissure, which is attributed to the plants beginning to lose their leaves.

Environmental Tracers

Meteoric Chloride

In general, chloride concentrations were lower in profiles beneath fissures than in profiles adjacent to fissures (figs. 2 and 3; table 3). Previous studies of the Hueco Bolson fissure showed low chloride concentrations ($\leq 110 \text{ g m}^{-3}$) in the upper 10 m in the profile immediately beneath the fissure and in profiles at 3 and 6 m from the fissure (Scanlon, 1992b). In this study, profiles beneath the Hueco Bolson fissure and 10 m distant from the fissure had low chloride concentrations, whereas chloride concentrations in the profile 50 m distant from the fissure were high ($\leq 5436 \text{ g m}^{-3}$) (fig. 2c). Chloride profiles in the vicinity of the Hueco Bolson fissure in this study extended to much greater depths (down to 26 m) than in the previous study (9.3 m) and showed an increase in chloride concentrations beneath the fissure from 2.5 g m^{-3} (14.1 m) to 1300 g m^{-3} (21.1 m), which probably marks the extent of flushing. The profile 10 m distant from the Hueco Bolson fissure also displays a chloride front that is sharper than that beneath the fissure and is also shallower (2.9 g m^{-3} at 11.0 m to 1792 g m^{-3} at 15.2 m).

In the Eagle Flat fissure, the zone of low chloride concentrations was restricted to beneath the fissure, whereas the profile 10 m distant from the fissure had high chloride concentrations (fig. 2f, i, and l). Chloride concentrations were low in the upper 9 m of the profile EFF35 0m and increased sharply to 5200 g m^{-3} within a 2-m-depth interval (fig. 2f). This shows that the vertical extent of leaching is less than that beneath the Hueco Bolson fissure. The chloride concentrations at depth beneath the Eagle Flat fissure were similar to those in the profile 10 m distant from the fissure. The vertical extent of chloride leaching and the degree of leaching is not the same in all profiles along Eagle Flat fissure. Low chloride concentrations ($\leq 800 \text{ g m}^{-3}$) were restricted to the upper 6 m of profile EFF88 0m beneath the fissure (fig. 2i). Although chloride concentrations in the third profile (EFF92 0m) beneath Eagle Flat fissure were much lower than that in the profile 10 m distant from the fissure (EFF96 10m) (fig. 2l), they were significantly higher than chloride

concentrations in the other two profiles beneath the fissure (fig. 2f and i) and represent incomplete flushing in this profile. Chloride profiles adjacent to Eagle Flat fissure had highest concentrations at the surface (up to 7916 g m^{-3} in EFF36 10m) and generally decreased with depth (fig. 2f, i, and l). The solute front in EFF35 0m correlates with a slight reduction in chloride in the profile 10 m distant from 4746 to 3405 g m^{-3} , which may reflect lateral flow. Sharp changes in chloride concentrations are also found in EFF59 10 m (reduction from 5509 to 3286 g m^{-3} at 15 m depth and increase to 8804 g m^{-3} with depth) (fig. 2i).

Chloride concentrations were fairly low ($\leq 273 \text{ g m}^{-3}$) throughout the profile in Ryan Flat fissure and increased gradually away from the fissure (fig. 3f; table 3). Maximum concentrations were 757 g m^{-3} at 1.71 m in the profile 10 m from the fissure and 2980 g m^{-3} at 1.28 m in the profile 50 m from the fissure. At depths ≥ 10 m, all three profiles had similar chloride concentrations (230 to 290 g m^{-3}). Chloride concentrations in the profile beneath Red Light Bolson fissure were low throughout ($\leq 100 \text{ g m}^{-3}$), with the exception of a local higher zone (150 to 844 g m^{-3}) from 4.5 to 6 m depth (fig. 3c). The chloride profile 50 m distant from the fissure had high chloride concentrations that ranged from 2991 g m^{-3} from 0.76 m to 1141 g m^{-3} at 8.2 m depth.

Isotopes

It was difficult to collect sufficient chloride for chlorine-36 analyses beneath the fissures. Where sufficient chloride was available, $^{36}\text{Cl}/\text{Cl}$ ratios were low (4.2×10^{-13} in EFF92 0m to 7.5×10^{-13} in RLB 0m) (fig. 6c and d; table 4) and do not indicate significant contribution from the bomb pulse. Previous studies at the Hueco Bolson site included analysis of the distribution of bomb pulse ^{36}Cl and showed that the $^{36}\text{Cl}/\text{Cl}$ ratios typical of the bomb pulse reached a maximum value of 65.6×10^{-13} (Scanlon, 1992b) and prebomb $^{36}\text{Cl}/\text{Cl}$ ratios were approximately 4.6×10^{-13} . A sample for $^{36}\text{Cl}/\text{Cl}$ analysis was also collected in a borehole 50 m distant from the Hueco Bolson fissure to determine if reductions in chloride concentrations at depth could be attributed to

preferential flow of water and dilution of chloride at depth. The ratio of $^{36}\text{Cl}/\text{Cl}$ was also low in this sample and does not give any indication of a bomb pulse component to the samples.

Soil samples from different depths were combined to obtain sufficient water for tritium analyses. High tritium concentrations were found in the profile beneath the Hueco Bolson fissure (5.2 to 21.7 TU) and also in the profile 10 m distant from the fissure (5.9 to 42.2 TU) (fig. 6a and b; table 4). Tritium concentrations remained high below the chloride front. High tritium levels were also found throughout the profile beneath Ryan Flat fissure (3.8 to 17.2 TU) (fig. 6e). Tritium concentrations beneath Ryan Flat fissure were higher in the upper 6 m (7.8 to 17.2 TU) than in the deeper section (11 to 25 m; 3.8 to 7.4 TU). High tritium concentrations were found beneath Eagle Flat fissure also (24.4 to 33.2 TU; fig. 6c; table 4).

Stable isotopes of oxygen and hydrogen were less enriched in the profile directly beneath Red Light Bolson fissure than in the profile 50 m distant from fissure (fig. 7; table 6). This suggests less evaporation of the water beneath the fissure than in the sediments distant from the fissure.

Electromagnetic Induction

Three fissures (Eagle Flat fissure, Ryan Flat fissure, and a section of Red Light Bolson fissure) showed higher apparent conductivity in the vicinity of the fissure relative to the surface adjacent to the fissure (fig. 8b, c, e, and f). In each case, the apparent conductivity measured with the EM31 instrument increased by a factor of approximately two in the vicinity of the fissure in both the vertical and horizontal dipole modes. The EM38 instrument was used only at Ryan Flat fissure, and apparent conductivity mapped with the EM38 also showed increases in the vicinity of the fissure by a factor of 2 in the horizontal dipole mode and by a factor of 3 in the vertical dipole mode (fig. 8g). The other fissures, Hueco Bolson fissure and another section of Red Light Bolson fissure, showed negligible variation in apparent conductivity in the vicinity of the fissure (fig. 8a and d). This section of the Red Light Bolson fissure differs from the other section in that the width-to-depth ratio is much less and probably represents a much older section of the fissure. This

older section is the area where the boreholes were drilled and samples were collected. Two transects were conducted on Eagle Flat fissure, one where there was a gully at the surface to mark the location of the fissure (fig. 8b) and a second parallel to the first but where there was no gully present (fig. 8c). The apparent conductivity along the second transect was similar to the first and indicates that this technique may be suitable for mapping increased subsurface water flux prior to development of surface collapse features associated with fissures.

Apparent conductivities measured with the EM31 were higher in the vertical dipole mode (VD) than in the horizontal dipole mode (HD) in all transects (fig. 8). Apparent conductivities measured in the vertical dipole mode ranged from a factor of 1.5 to 2 times higher than conductivities measured in the horizontal dipole mode. These data indicate that apparent conductivity increases with depth. The two transects (VD and HD) generally parallel each other. The increase in apparent conductivity with depth is also consistent with higher conductivities measured with the EM31 relative to those measured with the EM38 because of the differences in the exploration depths of these instruments.

The apparent electrical conductivity of a soil varies with water content, salt content, soil texture, mineralogy, and soil structure. Rhoades and others (1989) developed a model to describe the electrical conductivity of soil in terms of mobile (parallel pathway) and immobile (series pathway) water. The apparent electrical conductivity of the soil is proportional to the conductivity of the soil water when the solution conductivity is high relative to the solid phase conductance, generally at solution conductivities $\geq 400 \text{ mS m}^{-1}$. In this case, the following linear model can be used to describe variations in the apparent electrical conductivity of the soil

$$EC_a = EC_w \theta \tau + EC_s \quad (2)$$

where EC_w is the soil water conductivity, θ is volumetric water content, τ is the tortuosity, and EC_s is the surface conductance of the soil. This model applies when the water content is above a certain threshold value. Below this threshold value, EC_w is 0 and the apparent conductivity is controlled by the surface conductance.

The measured EC_a appears to be controlled mostly by variations in water content; therefore, this is not a very useful method for detecting higher subsurface water fluxes beneath fissures because water content varies also with texture and is not highly characteristic of fissured sediments. Low chloride concentrations provide a more distinctive signature of fissured sediments. The lack of variation in EC_a in some of the fissures (Hueco Bolson and a section of the Red Light Bolson) is attributed to water contents being too low to conduct electricity. This is supported by comparisons of downhole electrical conductivity measurements with an EM39 instrument and measured water content, which shows that the threshold water content is approximately 0.07 g g^{-1} (Paine and others, 1995).

DISCUSSION

Subsurface Water Movement in Fissured Sediments

The soil physics and soil water chemistry data are consistent and show that subsurface water fluxes are higher in fissured sediments than in nonfissured sediments. Higher water contents in Eagle Flat fissure that cannot be explained by textural variations, higher water potentials, and lower chloride concentrations in all profiles in fissured sediments relative to adjacent profiles in nonfissured sediments all indicate increased subsurface water movement beneath the fissures.

The fissures examined in this study represent a variety of stages of fissure development discussed by Larson and Péwé (1986). The Hueco Bolson and Ryan Flat fissures have large gullies and low width-to-depth ratios, which indicate that these fissures may be relatively young. In contrast, the sections of Eagle Flat and Red Light Bolson fissures studied have very small gullies and high width-to-depth ratios, which suggest that these fissures may be much older. The profiles drilled in the Eagle Flat fissure were restricted to the southernmost extent of the fissure because of lack of property access to drill in the main section of the fissure. This may explain the very localized effect of higher flux associated with Eagle Flat fissure, where the effect of the

fissure is not seen at 10 m distance, whereas the effect of increased flux is seen at 10 m in both the Hueco Bolson and Ryan Flat fissures. The main section of the Eagle Flat fissure may be similar to the Hueco Bolson and Ryan Flat fissures. With age, the fissured sediments may have sufficient time to dry out through increased evapotranspiration, which may explain the lower water potentials found in the Red Light Bolson fissure relative to all the other fissures and also the lack of response of the EM readings to this fissure. A more recently activated section of this fissure did show a response on the EM readings; however, boreholes could not be drilled in this section. Although the fissures may show that they dry out with age, this will not be seen in the chloride profiles because it takes a long time (up to thousands of years) for chloride to accumulate.

In addition to variations among fissures, differences in soil physics and chemical parameters were found within short intervals in the Eagle Flat fissure and indicate that there is substantial variability along individual fissures also. The different profiles in the Eagle Flat fissure indicate varying degrees of flushing of the soil water chloride.

Water Flux Estimates

Chloride profiles in fissured sediments cannot be used directly to estimate fluxes on the basis of the chloride mass balance approach because one of the assumptions of this approach is steady-state subsurface flow, which is not applicable to the fissures where flow is transient. The chloride in the profiles beneath the fissures may represent residual chloride, which reflects incomplete flushing of the chloride, and would not, therefore, represent the current flux through the sediments. This is most apparent in profiles EFF88 0m and EFF92 0m (fig. 8h and k). In contrast, the chloride in the profile EFF35 0m is much lower and probably represents more complete flushing (fig. 8e).

If the time that fluxes increased in fissured sediments was known, one could estimate the water fluxes from the depth of the chloride fronts found in Eagle Flat and Hueco Bolson fissures. The vegetation linear associated with Eagle Flat fissure is clearly visible in aerial photographs taken in 1957 (Jackson and others, 1993); however, the fissure may have been active for a much longer

time. Use of a minimum age for the initiation of the fissure will result in a maximum water velocity for subsurface flow in fissured sediments. If we assume that Eagle Flat fissure has been active for 50 yr and approximate the location of the chloride front to be 9 m, then the resultant water velocity would be 0.2 m yr^{-1} . An average gravimetric water content in the upper 9 m of EFF35 is 0.14 g g^{-1} and an average bulk density of 1.4 kg m^{-3} results in an average volumetric water content of $0.2 \text{ m}^3 \text{ m}^{-3}$, and the resultant water flux would be 40 mm yr^{-1} . This flux may be much greater than the actual water flux if the age of the fissure is much older. A similar analysis can be done for the Hueco Bolson fissure if we assume this fissure has been active for 50 yr and the midpoint of the chloride front is taken to be 17 m beneath the fissure and 14 m in the profile 10 m from the fissure. This results in velocities of 0.34 m yr^{-1} beneath the fissure and 0.28 m yr^{-1} 10 m from the fissure. The average volumetric water content is $0.14 \text{ m}^3 \text{ m}^{-3}$ beneath the fissure and $0.10 \text{ m}^3 \text{ m}^{-3}$ in the profile adjacent to the fissure (assuming a bulk density of 1.4 g m^{-3}) and results in a water flux of 48 mm yr^{-1} beneath the fissure and 28 mm yr^{-1} adjacent to the fissure. A portion of the water is flowing faster than represented by the chloride front, as indicated by the presence of bomb pulse tritium down to 17 m depth beneath the Hueco Bolson fissure and to 26 m in the profile 10 m distant from the Hueco Bolson fissure. However, the percentage of water flowing preferentially below the solute front cannot be determined with available data. Water velocities estimated from the tritium data range from 0.85 m yr^{-1} directly beneath the fissure to 0.56 m yr^{-1} 10 m distant from the fissure. This assumes that the tritium represents peak fallout in 1963 and uses the period between peak fallout and sampling (1994) to estimate the velocity. Using an average volumetric water content of $0.14 \text{ m}^3 \text{ m}^{-3}$ beneath the fissure and $0.08 \text{ m}^3 \text{ m}^{-3}$ in the profile 10 m distant from the fissure results in a range of fluxes from 120 mm yr^{-1} beneath the fissure to 45 mm yr^{-1} 10 m distant from the fissure. This represents a lower bound on the flux associated with preferential flow beneath the fissure because the maximum vertical extent of the bomb pulse signal is not known.

Piston versus Preferential Flow

Because surface fissures intercept drainage systems, water ponds on these features and focuses subsurface flow. Although some researchers refer to focused flow as a macroscopic scale preferential flow (Gee and Hillel, 1988), most workers restrict the term preferential flow to flow along macropores and/or unstable flow. Data collected in this study can be used to evaluate the relative importance of piston and preferential flow in fissured sediments.

In soils undergoing infiltration, an expression has been developed for the ratio of the velocities of the wetting and solute fronts based on one-dimensional analytical solutions for the flow and transport equations (Warrick and others, 1971):

$$R_{wf} = \frac{\theta_{wet} - \theta_{dry}}{\theta_{wet}} \quad (3)$$

The above analysis indicates that under piston flow conditions the wetting front should precede the solute front by an amount equal to the amount of water in the profile initially prior to infiltration. This was found in water potential and chloride profiles measured in an area of Australia that had been cleared of mallee vegetation (Jolly and others, 1989). The sharp chloride fronts in some of the profiles in Eagle Flat fissure suggest piston flow. If we assume that the water content in the profile 10 m distant from the fissure (EFF36 10m) represents the initial water content (θ_{dry}) in the upper 9.7 m of the profile beneath the fissure (EFF35 0m), then we should expect a much greater separation between the wetting front and chloride front than what is found. An alternative explanation for the sharp chloride front beneath the Eagle Flat fissure may be provided by the natural capillary barriers created by the distinct layering of sediments in the profile. The depth of the solute front corresponds approximately to an increase in sand content from 13 to 65%. In the presence of natural capillary barriers, water would accumulate on top of the coarse-textured layer until the water potential increased sufficiently to overcome the water-entry pressure of the underlying coarse layer. While water is accumulating on the coarse layer, the separation between the wetting and solute fronts would decrease. In addition, the above analysis of the relative positions of wetting and solute fronts was based on one-dimensional flow; however, water flow

beneath Eagle Flat fissure may be two-dimensional. Reductions in chloride in EFF36 10m at depth may be related to lateral flow along a capillary barrier (fig. 2f). Low chloride concentrations at approximately 5 m depth in EFF88 0m and EFF92 0m (fig. 2i and l) may also reflect lateral flow along a capillary barrier because a sand layer is found at this depth.

The sharpness of the chloride fronts found in one of the profiles beneath Eagle Flat fissure and also in the profiles in the Hueco Bolson fissure and the profile 10 m distant from the Hueco Bolson fissure suggests predominantly piston-type flow. In contrast, other profiles (EFF88 0m and EFF92 0m) along Eagle Flat fissure represent partial flushing of chloride and preferential flow. EFF35 0m is located within a gully, whereas the other two profiles were drilled outside gullies. Bomb pulse tritium found below the depth of the chloride front in the profiles beneath and 10 m distant from the Hueco Bolson fissure indicates that a component of the water is flowing preferentially.

Evaluation of Different Techniques to Estimate Flow in Fissured Sediments

Chloride concentration in soil water is a reliable indicator of subsurface flow in fissured sediments. All profiles beneath the fissure and in some cases those 10 m distant from the fissure had low chloride concentrations. Although chloride in soil water takes a long time (up to thousands of years) to accumulate, chloride is extremely soluble and one period of high water flux can readily flush all the chloride out of the profile. Because of the above, the low chloride in fissured sediments may be a relict of higher fluxes in the past and may not represent current conditions. This may be the case for the old fissures that are being filled with sediment.

High soil water potentials also seem to correspond well to fissured zones. Unlike the chloride profiles that may be relicts in some of the old fissures of higher fluxes in the past, the water potentials probably represent current conditions. Although the water potentials in profiles beneath the fissures are much higher than in adjacent profiles, the differences in water potential may not necessarily represent large differences in water content. This is particularly true for the profile beneath Red Light Bolson fissure and suggests that the sediments in this fissure are drying.

The relationship between water potential and water content is defined by the water retention function. Information on these functions would be required to assess the significance of the water potential differences with respect to water storage differences. It is likely that the water potentials measured in the Hueco Bolson fissure and the profile 10 m distant are within the steep section of the water retention function, where water potential changes rapidly without much change in water content; therefore, water storage beneath the Hueco Bolson fissure may not be markedly different from the profile 50 m distant. Water potential differences between the profiles beneath Eagle Flat fissure and the profiles 10 m distant are associated with water content differences that are not related to variations in texture; therefore, these water potential differences reflect significant differences in water storage.

Tritium is also a good indicator of preferential flow associated with fissured sediments. Tritium was detected in many fissured profiles down to the base of the profile; therefore, the vertical extent of the tritium cannot be determined. Stable isotopes of O and H also suggest less enrichment of the water directly beneath the fissures, which is consistent with the chloride and water potential data.

The chlorine-36 data indicated little bomb pulse signature in the profiles through the fissured sediments. This may result from dilution of the bomb pulse signature with old residual chloride that was incompletely flushed from the system. Because zones of high flux are associated with low chloride concentrations, it is difficult to collect sufficient chloride for analysis of chlorine-36; therefore, chlorine-36 is not suitable for areas of high flux.

Water content alone is not a very useful indicator of flow in fissured sediments because variations in water content may reflect differences in soil texture. However, analysis of water content and texture data can be used to evaluate zones of higher water flux, such as those at Eagle Flat fissure. Electromagnetic induction is of limited use in defining fissure flow because the primary control on apparent conductivity variations is water content, and water content variations are not very distinctive of fissures. In natural interfluvial settings in arid regions, water fluxes and resultant water contents are extremely low and the conductivity corresponding to the water is

essentially zero. This corresponds to the threshold water contents of Rhoades and others (1976). Slightly higher water contents associated with Eagle Flat fissure register as higher conductivity.

CONCLUSIONS

Higher water potentials and lower chloride concentrations in fissured sediments than those in adjacent nonfissured sediments indicate higher water fluxes beneath fissures. Sharp water potential and chloride fronts were found beneath two of the fissures in the upper 20-m zone, which indicates that most of the flow was restricted to this depth. These sharp fronts are attributed to natural capillary barriers beneath one of the fissures. Water flux estimates based on the position of the chloride front and an assumed age of the Hueco Bolson fissure of 50 yr ranged from 28 to 48 mm yr⁻¹. High tritium levels were found throughout the fissured profiles (to maximum depth of 26.4 m) and in some cases in the profiles 10 m distant from the fissure also, which indicates post-1952 water. High tritium levels beneath the chloride front in one fissure indicate that some of the water is flowing preferentially. Minimum estimates of water flux based on the tritium data ranged from 45 to 120 mm yr⁻¹. Stable isotopes of oxygen and hydrogen were less enriched beneath the fissure than in adjacent sediments, which is consistent with higher fluxes beneath the fissure. Apparent conductivities measured with an EM31 instrument were higher across two fissures, whereas the other two fissures did not show any variation in apparent conductivity. The higher conductivity beneath some fissures results from higher water content.

Multiple independent lines of evidence indicate that subsurface water fluxes are higher beneath fissures; however, the effectiveness of the various techniques in delineating fissure flow varied. Water potential and chloride profiles differed markedly between fissured and nonfissured sediments. Tritium is also a good indicator of preferential flow in fissured sediments. Predawn plant water potential differences in fissures and adjacent to fissures were significant in only two of the fissures. Apparent conductivities did not vary systematically between fissures and nonfissured sediments.

Variations in measured parameters were found among fissures and were attributed to the different stages of maturity of the fissures examined. As fissures mature, they are filled with sediment and no longer actively concentrate surface runoff and therefore should dry out. Multiple profiles drilled in one fissure indicate that there are also variations in subsurface flux along fissures.

ACKNOWLEDGMENTS

This project was funded by the National Low-Level Radioactive Waste Management Program, U.S. Department of Energy, Assistant Secretary for Environmental Management, under DOE Idaho Operations Office Contract No. DE-AC07-95ID 13233 and Interagency Contract No. 94-0304. The authors gratefully acknowledge the cooperation of the landowners (Deron Kasparian and El Paso Water Utilities). Particle size analyses were conducted by the University of Wisconsin Soil Laboratory. Figures were drafted by John Ames under the supervision of Richard L. Dillon. Word processing was by Susan Lloyd, and editing was by Bobby Duncan.

REFERENCES

- Allison, G.B., and Hughes, 1978, The use of environmental chloride and tritium to estimate total recharge to an unconfined aquifer: *Australian Journal of Soil Research*, v. 16, p. 181–195.
- Allison, G.B., Stone, W.J., and Hughes, M.W., 1985, Recharge in karst and dune elements of a semi-arid landscape as indicated by natural isotopes and chloride: *Journal of Hydrology*, v. 76, p. 1–26.
- Baumgardner, R.W., Jr., and Scanlon, B.R., 1992, Surface fissures in the Hueco Bolson and adjacent basins, West Texas: The University of Texas at Austin, Bureau of Economic Geology Geological Circular 92-2, 40 p.

- Bentley, H.W., Phillips, F.M., and Davis, S.N., 1986, ^{36}Cl in the terrestrial environment, *in* Fritz, P., and Fontes, J.-C., eds., Handbook of environmental isotope geochemistry: New York, Elsevier Science, v. 2b, p. 422–475.
- Boling, J.K., 1986, Earth-fissure movements in south-central Arizona, U.S.A., *in* Johnson, A.I., Carbognin, L., and Ubertini, L., eds., Land subsidence: Proceedings of the Third International Symposium on Land Subsidence, Venice, Italy, March 19–25, 1984, International Association of Hydrological Sciences Publication No. 151, p. 757–766.
- Campbell, G.S., 1985, Soil physics with BASIC: Transport models for soil-plant systems: Elsevier, New York, 150 p.
- Edmunds, W.M., and Walton, N.R.G., 1980, A geochemical and isotopic approach to recharge evaluation in semi-arid zones: past and present, *in* Arid zone hydrology, investigations with isotope techniques: International Atomic Energy Agency, Vienna, IAEA-AG-158/4, p. 47–68.
- Elmore, D., Conard, N.J., Kubik, P.W., and Fabryka-Martin, J., 1984, Computer controlled isotope ratio measurements and data analysis: Nuclear Instruments and Methods in Physics Research, Section B, v. 5, p. 233–237.
- Folk, R.L., 1974, Petrology of sedimentary rocks: Hemphill, Austin, Texas, 182 p.
- Gee, G.W., and Bauder, J.W., 1982, Particle-size analysis, *in* Page, A.L., ed., Methods of soil analysis, part 2, Chemical and mineralogical methods: Madison, Wisconsin, American Society of Agronomy, p. 383–410.
- Gee, G.W., and Hillel, D., 1988, Groundwater recharge in arid regions: review and critique of estimation methods: Hydrological Processes, v. 2, p. 255–266.
- Ingraham, N.L., and Shadel, C., 1992, A comparison of toluene distillation and vacuum/heat method for extracting soil water for stable isotopic analysis: Journal of Hydrology, v. 140, p. 371–387.
- Jackson, M.L.W., Langford, R.P., and Whitelaw, M.J., 1993, Basin-fill stratigraphy, Quaternary history, and paleomagnetism of the Eagle Flat study area, Southern Hudspeth County, Texas: The University of Texas at Austin, Bureau of Economic Geology, report prepared for the

- Texas Low-Level Radioactive Waste Disposal Authority under contract no. IAC(92-93)-0910, 137 p.
- Jolly, I.D., Cook, P.G., Allison, G.B., and Hughes, M.W., 1989, Simultaneous water and solute movement through an unsaturated soil following an increase in recharge: *Journal of Hydrology*, v. 111, p. 391–396.
- Lang, A.R.G., 1967, Osmotic coefficients and water potentials of sodium chloride solutions from 0° to 40° C, *Australian Journal of Chemistry*, v. 20, p. 2017–2023.
- Larson, M.K., and Péwé, T.L., 1986, Origin of land subsidence and earth fissuring, northeast Phoenix, Arizona: *Association of Engineering Geologists Bulletin*, v. 23, no. 2, p. 139–165.
- McNeill, J.D., 1992, Rapid, accurate mapping of soil salinity by electromagnetic ground conductivity meters, *in* *Advances in measurement of soil physical properties: Bringing theory into practice: Soil Science Society of America Special Publication No. 30*, p. 209–229.
- Paine, J.G., Goldsmith, R.S., and Scanlon, B.R., 1995, Electrical conductivity and gamma ray response to clay, water and chloride content in fissured sediments, Trans-Pecos, Texas: Bureau of Economic Geology, The University of Texas at Austin, final report prepared for the National Low-Level Radioactive Waste Management Program, U.S. Department of Energy, Assistant Secretary for Environmental Management, under DOE Idaho Operations Office Contract No. DE-AC07-95ID 13223 and Interagency Contract No. 94-0304, 44 p.
- Rhoades, J.D., Raats, P.A.C., and Prather, R.J., 1976, Effects of liquid-phase electrical conductivity, water content, and surface conductivity on bulk soil electrical conductivity: *Soil Science Society of America Journal*, v. 40, p. 651–655.
- Robinson, G.M., and Peterson, D.E., 1962, Notes on earth fissures in southern Arizona: U.S. Geological Survey Circular 466, 7 p.
- Scanlon, B.R., 1992a, Evaluation of liquid and vapor water flow in desert soils based on chlorine-36 and tritium tracers and nonisothermal flow simulations: *Water Resources Research*, v. 28, p. 185–197.

- Scanlon, B.R., 1992b, Moisture and solute flux along preferred pathways characterized by fissured sediments in desert soils: *Journal of Contaminant Hydrology*, v. 10, p. 19–46.
- Scanlon, B.R., 1994, Water and heat fluxes in desert soils 1. Field studies: *Water Resources Research*, v. 30, p. 709–719.
- Schumann, H. H., Cripe, L. S., and Laney, R. L., 1986, Land subsidence and earth fissures caused by groundwater depletion in southern Arizona, U.S.A., *in* Johnson, A. I., Carbognin, L., and Ubertini, L., eds., *Land subsidence: Proceedings of the Third International Symposium on Land Subsidence, Venice, Italy, March 19–25, 1984*, International Association of Hydrological Sciences Publication No. 151, p. 841–851.
- Slaff, Steven, 1989, Patterns of earth-fissure development: examples from Picacho Basin, Pinal County, Arizona: *Arizona Geology*, v. 19, no. 3, p. 4–5.
- U.S. Department of Agriculture, *Soil taxonomy*: Washington, D.C., 754 p.
- Warrick, A.W., Biggar, J.W., and Nielsen, D.R., 1971, Simultaneous solute and water transfer for an unsaturated soil: *Water Resources Research*, v. 7, p. 1216–1225.

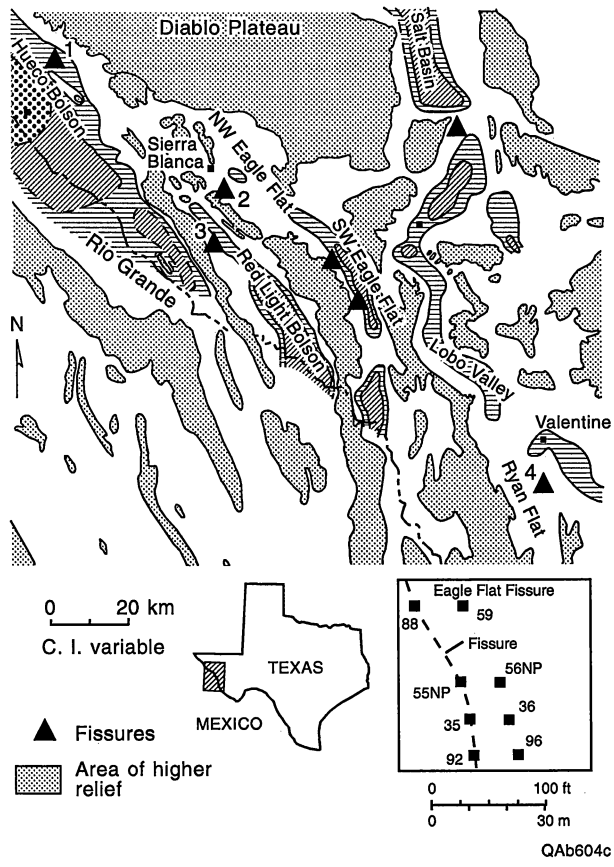


Figure 1. Map of fissures in study area: (1) Hueco Bolson, (2) Eagle Flat, (3) Red Light Bolson, and (4) Ryan Flat (modified from Baumgardner and Scanlon, 1992).

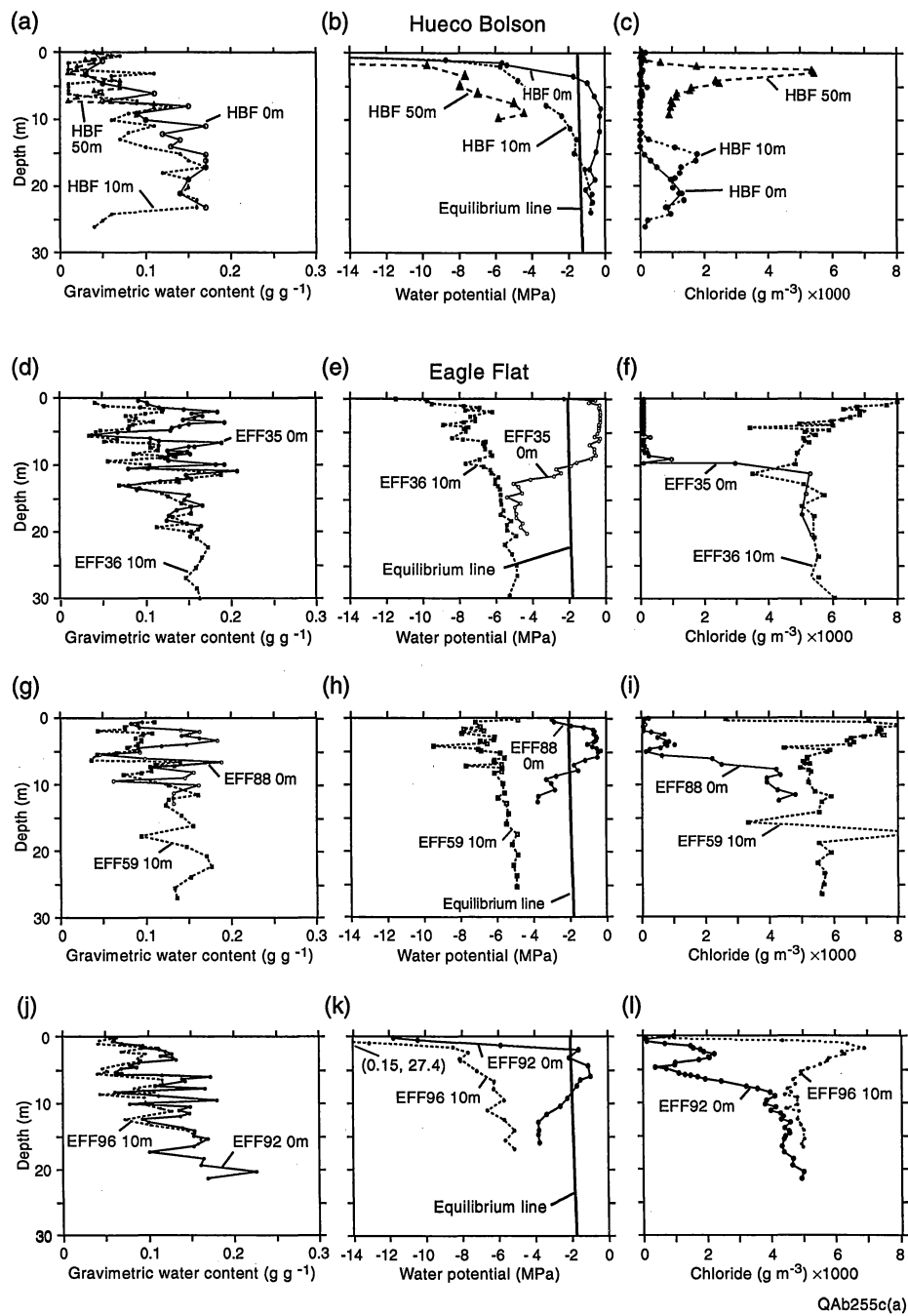
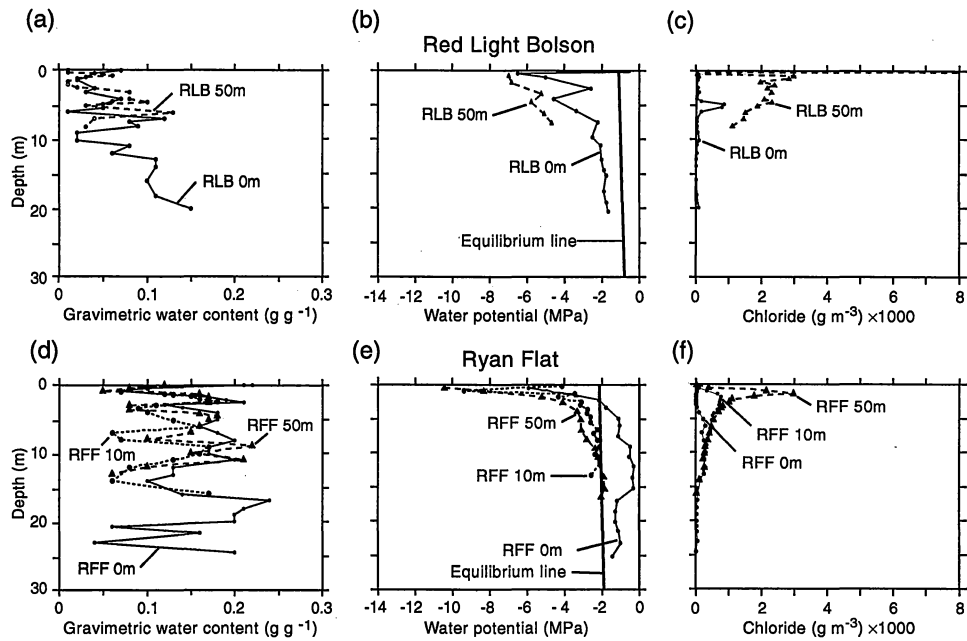


Figure 2. Profiles of texture, gravimetric water content, water potential, and chloride concentrations in and adjacent to Hueco Bolson and Eagle Flat fissures.



QAb255c(b)

Figure 3. Profiles of texture, gravimetric water content, water potential, and chloride concentrations in and adjacent to Red Light Bolson and Ryan Flat fissures.

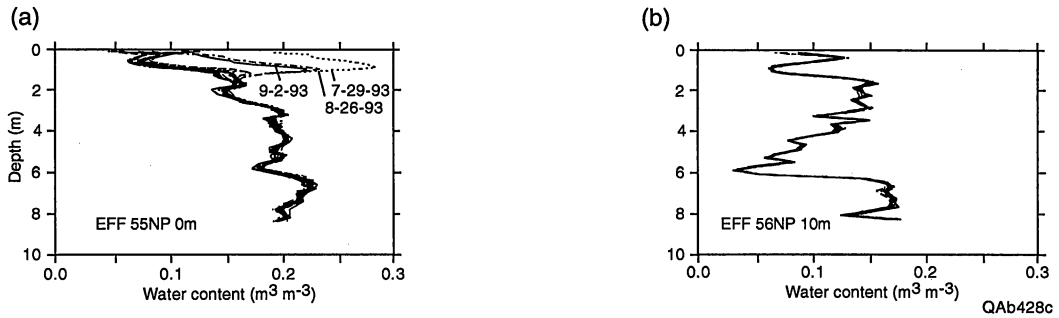
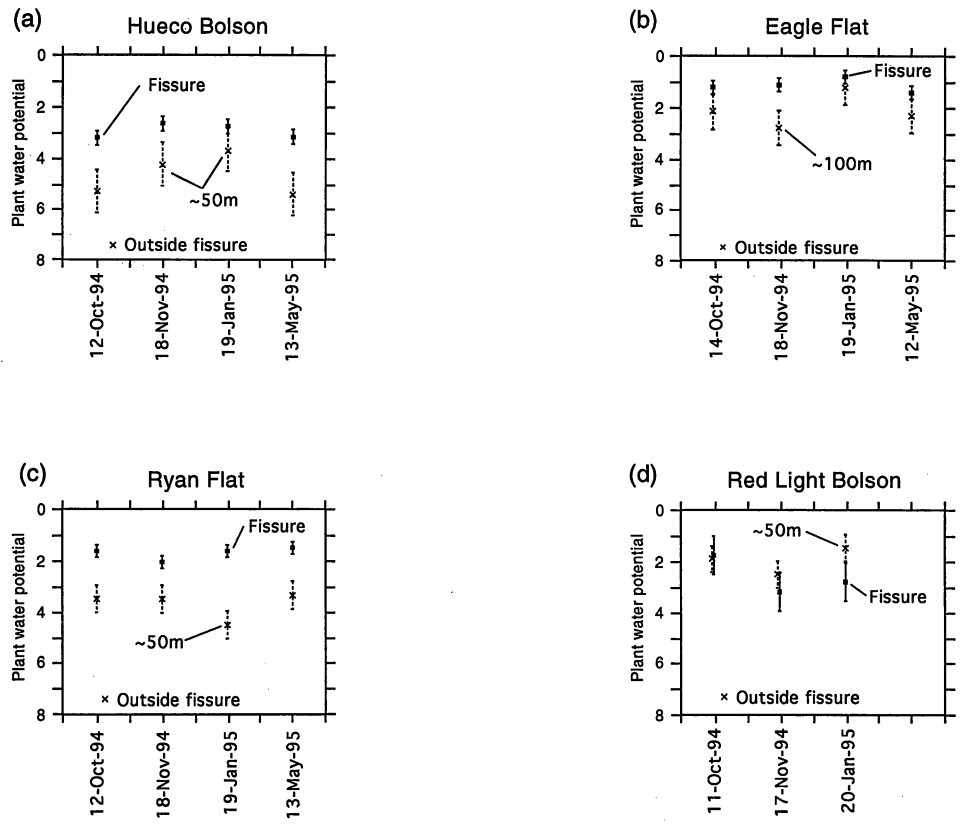


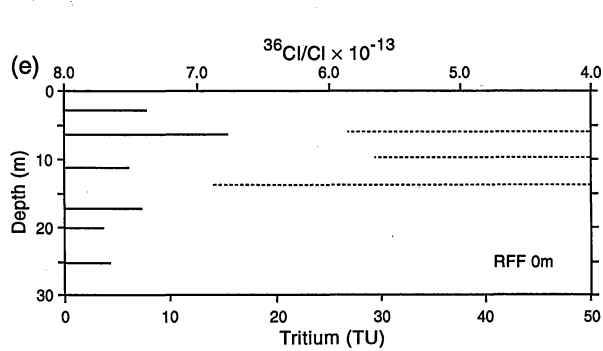
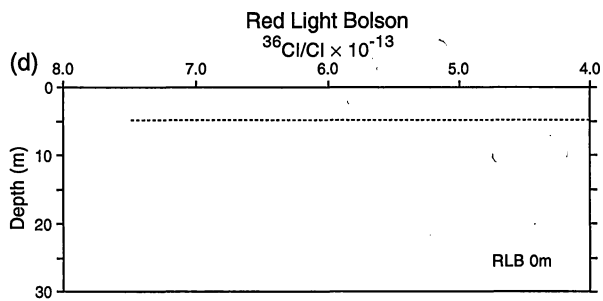
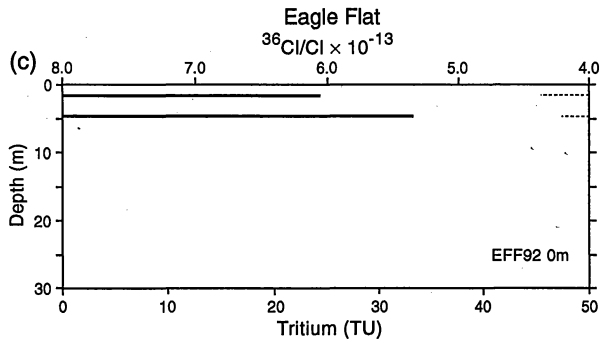
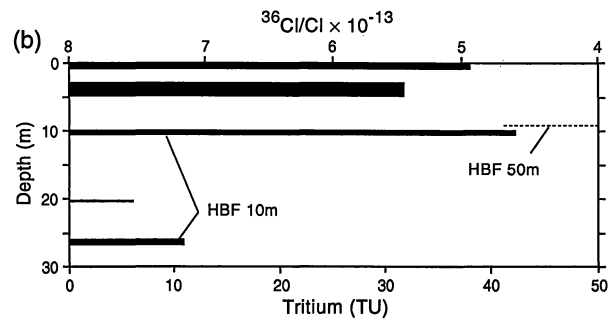
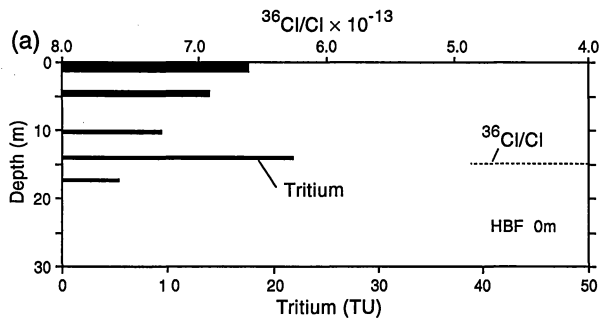
Figure 4. Variation in water content with depth and time in neutron probe access tubes in and 10 m distant from Eagle Flat fissure. Water content was monitored approximately monthly from June 1993 to August 1994 and in February and May, 1995.



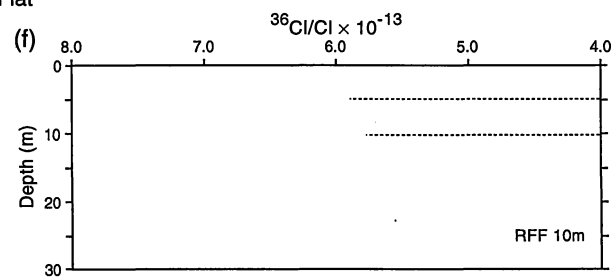
QAb496c

Figure 5. Predawn plant water potentials measured in and adjacent to fissures.

Hueco Bolson



Ryan Flat



QAb348c

Figure 6. Variations in ^3H and $^{36}\text{Cl}/\text{Cl}$ in profiles in and adjacent to fissures.

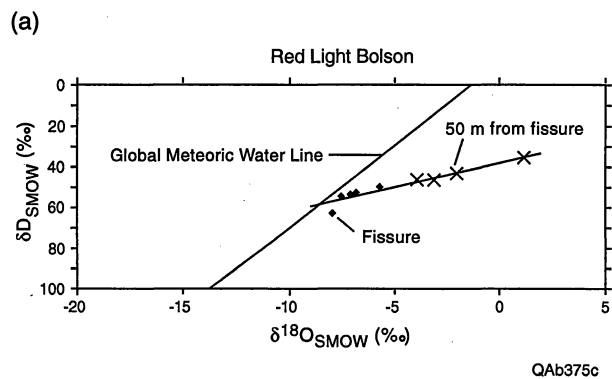
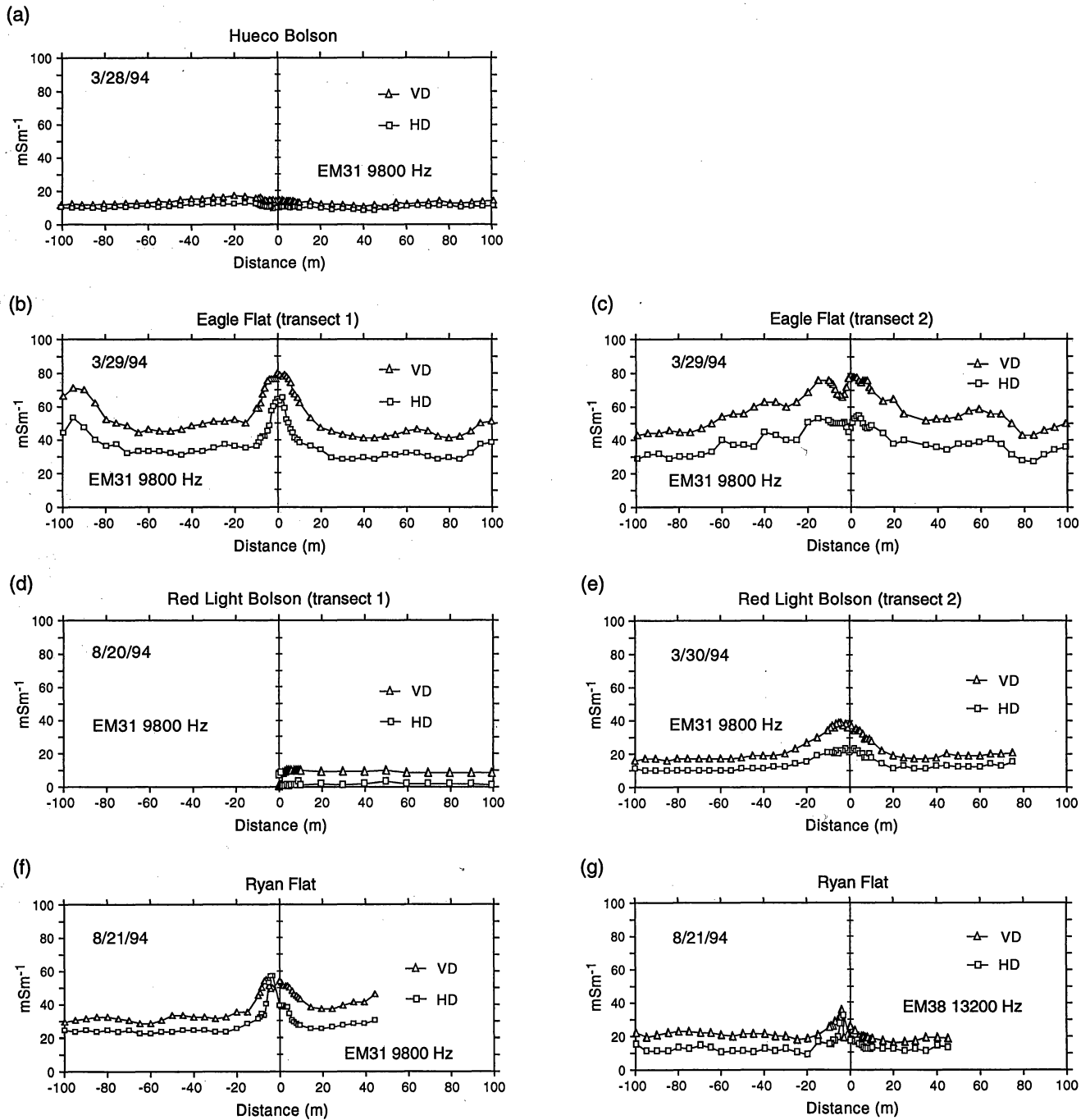


Figure 7. Stable isotopes of oxygen and hydrogen for a profile beneath Red Light Bolson fissure and 50 m distant from the fissure.



QAb349c

Figure 8. Electromagnetic transects across fissures.

Table 1. Texture and gravimetric water content of soil samples collected beneath and adjacent to fissures.

Borehole number	Depth (m)	Gravel %	Sand %	Silt %	Clay %	Soil texture	Water content g/g
HBF 0m	0.03	1	42	36	21	loam	0.04
	2.82	42	33	13	11	msG	0.03
	6.13	10	42	29	18	gM	0.11
	7.19	58	21	12	9	msG	0.05
	8.05	0	39	32	29	clay loam	0.15
	9.11	1	65	12	22	sandy clay loam	0.09
	11.03	1	54	16	30	sandy clay loam	0.17
	13.12	0	16	54	29	silty clay loam	0.14
	16.17	0	25	27	48	clay	0.17
	21.08	1	52	11	37	sandy clay	0.14
R	-0.67	0.07	0.24	0.83			
R ²	0.45	0.01	0.06	0.68			
HBF 10m	0.03	1	52	29	18	sandy loam	0.03
	1.65	72	12	8	7	mG	0.01
	3.14	6	36	33	25	gM	0.11
	5.67	71	19	6	3	msG	0.01
	8.15	0	44	23	33	clay loam	0.13
	10.07	4	62	21	13	(g)mS	0.06
	14.14	0	46	30	24	loam	0.10
	17.13	2	38	17	43	clay	0.17
	23.23	1	50	20	30	sandy clay loam	0.16
	26.14	0	85	5	10	loamy sand	0.04
R	-0.63	0.11	0.44	0.94			
R ²	0.40	0.01	0.19	0.89			
HBF 50m	0.03	1	57	28	14	sandy loam	0.04
	3.11	80	14	3	3	G	0.01
	7.22	76	16	3	4	msG	0.01
	8.24	0	39	23	38	clay loam	0.11
	R	-0.80	0.52	0.69	1.00		
R ²	0.64	0.27	0.48	1.00			
EFF 35 0m	0.29	2	41	30	27	clay loam	0.10
	0.59	0	40	36	24	loam	0.11
	0.90	0	49	30	22	loam	0.11
	1.26	1	55	25	19	sandy loam	0.12
	1.57	1	44	31	24	loam	0.15
	1.87	0	31	46	24	loam	0.19
	2.18	0	22	53	25	silt loam	0.16
	2.58	1	30	45	24	loam	0.17
	2.82	0	36	42	22	loam	0.16
	3.12	1	48	33	18	loam	0.15
	3.43	0	31	47	22	loam	0.20
	3.73	1	37	37	25	loam	0.15
	4.10	2	43	34	21	loam	0.14
	4.37	4	46	29	22	(g)sM	0.13
	4.68	2	50	26	21	sandy clay loam	0.13
	4.95	33	49	11	7	msG	0.07
	5.41	0	90	6	4	sand	0.04
	5.93	4	51	25	20	(g)mS	0.11
	6.23	0	53	18	30	sandy clay loam	0.12
	6.54	0	21	45	34	clay loam	0.19

Table 1. Texture and gravimetric water content of soil samples collected beneath and adjacent to fissures.

Borehole number	Depth (m)	Gravel %	Sand %	Silt %	Clay %	Soil texture	Water content g/g
EFF 35 0m	7.09	0	28	47	25	loam	0.16
	7.76	0	29	40	30	clay loam	0.15
	8.21	0	14	42	44	silty clay	0.16
	8.73	0	42	36	22	loam	0.13
	9.16	0	42	31	26	loam	0.13
	9.68	0	13	52	34	silty clay loam	0.19
	10.32	0	65	18	17	sandy loam	0.08
	10.71	0	3	66	30	silty clay loam	0.21
	11.32	0	31	49	20	loam	0.15
	11.84	0	24	57	19	silt loam	0.16
	12.88	0	50	32	18	loam	0.08
	13.40	2	26	38	33	clay loam	0.09
	14.31	0	15	58	27	silty clay loam	0.15
	14.95	0	18	60	21	silt loam	0.15
	15.86	1	18	60	22	silt loam	0.17
	16.54	3	19	56	23	(g)sM	0.14
	17.42	0	32	48	20	loam	0.13
	18.09	8	16	48	29	gM	0.13
	18.91	0	15	56	29	silty clay loam	0.17
	19.46	0	13	60	27	silty clay loam	0.17
20.47	0	19	58	23	silt loam	0.16	
R	-0.35	-0.75	0.77	0.53			
R^2	0.13	0.57	0.59	0.29			
	0.59	0	36	19	45	clay	0.05
	1.05	0	54	23	23	sandy clay loam	0.06
	1.36	0	32	24	44	clay	0.10
	1.97	0	30	21	48	clay	0.12
	2.27	0	26	23	50	clay	0.10
	2.58	0	28	21	50	clay	0.08
	2.91	0	35	24	41	clay	0.09
	3.22	0	50	20	30	sandy clay loam	0.09
	3.52	0	27	20	52	clay	0.11
	3.83	1	39	24	37	clay loam	0.09
	4.13	1	47	20	33	sandy clay loam	0.09
	4.47	2	45	20	32	sandy clay loam	0.09
	4.77	1	66	12	21	sandy clay loam	0.05
	5.07	1	62	20	17	sandy loam	0.05
	5.47	0	72	14	14	sandy loam	0.04
	6.02	0	54	25	22	sandy clay loam	0.07
	6.32	0	63	19	18	sandy loam	0.06
	6.63	0	26	28	45	clay	0.11
	6.93	0	25	23	52	clay	0.12
	7.30	0	23	24	52	clay	0.11
	7.70	0	26	27	47	clay	0.12
	8.21	0	41	23	36	clay loam	0.09
	8.67	0	5	39	57	clay	0.14
	9.25	0	31	44	25	loam	0.06
	9.86	0	16	39	45	clay	0.11
	10.35	0	24	34	43	clay	0.11
	10.81	0	4	27	69	clay	0.17
	11.29	0	34	16	49	clay	0.19
	11.96	0	23	17	60	clay	0.14

Table 1. Texture and gravimetric water content of soil samples collected beneath and adjacent to fissures.

Borehole number	Depth (m)	Gravel %	Sand %	Silt %	Clay %	Soil texture	Water content g/g
EFF 36 10m	12.36	0	26	19	55	clay	0.14
	12.85	0	45	24	30	clay loam	0.07
	13.27	1	34	27	39	clay loam	0.10
	14.10	0	24	27	48	clay	0.12
	14.52	0	17	29	54	clay	0.13
	15.47	0	19	24	58	clay	0.15
	16.08	0	18	24	58	clay	0.16
	17.02	0	17	24	60	clay	0.16
	17.63	0	27	23	50	clay	0.14
	18.58	1	19	25	55	clay	0.15
	19.19	0	29	25	46	clay	0.12
	19.95	0	20	23	57	clay	0.16
	20.86	0	13	26	60	clay	0.16
	22.17	1	11	20	68	clay	0.18
	23.76	0	13	29	58	clay	0.17
	25.31	0	13	31	55	clay	0.16
	26.87	0	10	32	58	clay	0.15
	28.42	0	10	36	54	clay	0.17
29.98	0	13	32	55	clay	0.17	
R		-0.25	-0.84	0.26	0.88		
R ²		0.06	0.70	0.07	0.78		
EFF 59 10m	0.22	0	32	26	42	clay	0.11
	0.53	0	41	20	39	clay loam	0.09
	0.92	0	45	21	34	clay loam	0.07
	1.29	0	45	22	33	clay loam	0.07
	1.56	10	61	11	18	(g)mS	0.04
	1.90	0	27	26	46	clay	0.10
	2.20	0	24	26	49	clay	0.09
	2.60	0	27	24	49	clay	0.09
	2.84	1	31	24	44	clay	0.09
	3.15	0	36	25	38	clay loam	0.09
	3.45	1	36	27	36	clay loam	0.09
	3.76	0	29	35	36	clay loam	0.09
	4.06	2	45	22	31	sandy clay loam	0.08
	4.58	0	24	33	43	clay	0.08
	4.88	1	53	22	24	sandy clay loam	0.06
	5.19	5	73	9	14	(g)mS	0.04
	5.95	63	22	6	8	msG	0.03
	6.26	0	6	38	56	clay	0.14
	6.56	1	28	29	41	clay	0.11
	6.87	0	19	26	55	clay	0.13
	6.96	0	32	23	44	clay	0.10
	7.51	1	20	37	42	clay	0.10
7.90	0	35	27	38	clay loam	0.09	
8.21	0	49	23	29	sandy clay loam	0.07	
9.76	0	17	32	51	clay	0.12	
11.13	0	7	29	63	clay	0.16	
11.83	0	13	21	66	clay	0.12	
12.69	2	30	24	45	clay	0.12	
14.24	0	17	28	55	clay	0.14	
15.80	0	16	26	58	clay	0.15	
17.35	0	24	42	34	clay loam	0.09	

Table 1. Texture and gravimetric water content of soil samples collected beneath and adjacent to fissures.

Borehole number	Depth (m)	Gravel %	Sand %	Silt %	Clay %	Soil texture	Water content g/g
	18.91	0	12	32	56	clay	0.15
	20.46	0	16	26	58	clay	0.17
	22.01	0	12	28	60	clay	0.17
	25.21	0	19	34	47	clay	0.13
	26.68	0	19	37	44	clay	0.13
	R	-0.42	-0.80	0.58	0.91		
	R ²	0.18	0.64	0.33	0.82		
EFF 88 0m	0.22	0	41	26	32	clay loam	0.09
	0.53	0	31	27	41	clay	0.08
	1.10	1	44	22	33	clay loam	0.09
	1.41	0	27	29	43	clay	0.14
	1.71	0	37	23	40	clay	0.16
	2.02	0	27	23	50	clay	0.15
	2.34	0	26	21	52	clay	0.14
	2.96	1	36	27	37	clay loam	0.18
	3.57	1	28	27	44	clay	0.15
	3.89	2	37	29	32	clay loam	0.12
	4.21	4	55	18	23	(g)mS	0.09
	4.52	3	57	18	22	(g)mS	0.09
	4.82	0	58	23	18	sandy loam	0.09
	5.13	0	89	4	7	sand	0.04
	5.77	0	63	20	17	sandy loam	0.10
	6.29	0	12	37	51	clay	0.19
	7.06	0	39	21	39	clay loam	0.10
	7.84	0	19	37	43	clay	0.15
	8.59	0	17	33	50	clay	0.14
	9.15	0	10	32	59	clay	0.06
9.73	0	58	24	18	sandy loam	0.16	
10.95	0	28	24	48	clay	0.13	
11.65	3	20	26	52	(g)sM	0.13	
12.50	0	16	26	58	clay	0.13	
	R	-0.30	-0.50	0.55	0.43		
	R ²	0.09	0.25	0.30	0.18		
EFF 92	0.79	0	41	26	33	clay loam	0.06
	2.62	0	29	21	50	clay	0.13
	4.88	0	50	29	21	loam	0.07
	8.35	0	70	14	16	sandy loam	0.06
	12.44	0	36	24	40	clay loam	0.09
	15.42	0	20	21	59	clay	0.17
	17.40	0	38	22	40	clay loam	0.10
	20.44	0	16	13	71	clay	0.23
	R		-0.84	-0.55	0.94		
	R ²		0.70	0.30	0.88		
RLB 0m	0.03	32	44	15	9	msG	0.07
	1.46	52	27	12	9	msG	0.02
	6.04	62	28	5	6	msG	0.01
	8.15	0	31	46	23	loam	0.09
	10.23	65	18	9	8	mG	0.02
	16.03	0	32	44	24	loam	0.10
	R	-0.97	0.58	0.91	0.89		

Table 1. Texture and gravimetric water content of soil samples collected beneath and adjacent to fissures.

Borehole number	Depth (m)	Gravel %	Sand %	Silt %	Clay %	Soil texture	Water content g/g
	R ²	0.94	0.34	0.82	0.80		
RLB 50m	0.03	0	25	49	26	loam	0.01
	0.76	9	24	38	29	gM	0.06
	2.48	61	25	7	7	msG	0.02
	3.22	4	41	25	31	(g)sM	0.08
	6.17	0	15	32	53	clay	0.13
	R	-0.47	-0.24	0.00	0.87		
	R ²	0.22	0.06	0.00	0.76		
RFF 0m	0.03	0	35	23	42	clay	0.21
	0.98	0	45	31	24	loam	0.07
	2.50	0	14	10	76	clay	0.21
	2.90	1	38	28	33	clay loam	0.12
	6.05	0	22	15	63	clay	0.16
	9.10	0	18	39	43	clay	0.17
	11.02	0	21	40	38	clay loam	0.20
	14.16	41	39	12	8	msG	0.10
	17.01	0	12	19	69	clay	0.24
	20.06	0	24	31	45	clay	0.20
	20.85	15	68	4	13	gmS	0.06
	21.67	0	27	43	30	clay loam	0.16
	23.10	37	53	5	6	msG	0.04
24.63	0	23	20	57	clay	0.20	
	R	-0.66	-0.88	0.36	0.84		
	R ²	0.43	0.77	0.13	0.71		
RFF 10m	0.03	3	33	21	43	(g)sM	0.22
	0.82	1	29	43	28	clay loam	0.07
	2.47	0	18	21	61	clay	0.18
	3.41	0	48	25	27	sandy clay loam	0.09
	6.13	0	27	19	54	clay	0.16
	8.09	4	65	11	20	(g)mS	0.07
	10.09	0	29	18	53	clay	0.16
14.07	7	61	18	14	gmS	0.06	
	R	-0.39	-0.70	-0.19	0.84		
	R ²	0.15	0.49	0.04	0.71		
RFF 50m	0.03	8	70	10	11	gmS	0.12
	0.87	0	57	23	20	sandy clay loam	0.05
	2.15	0	23	22	54	clay	0.17
	6.05	0	32	21	47	clay	0.16
	7.94	0	53	24	23	sandy clay loam	0.10
	10.99	0	19	25	56	clay	0.21
	R	-0.13	-0.80	0.14	0.83		
	R ²	0.02	0.64	0.02	0.69		

Table 2. Gravitational water content, chloride concentrations, water flux, water velocity, age, cumulative chloride, and cumulative water content of soil samples.

Borehole number	Depth (m)	Gravitational potential (MPa)	Water potential (MPa)	Total potential (MPa)	Depth (m)	Osmotic potential (MPa)
HBF 0m	0.46	-1.47	-15.86	-17.33		
	1.49	-1.46	-5.60	-7.06		
	1.92	-1.45	-5.34	-6.79		
	3.48	-1.44	-1.69	-3.13		
	4.54	-1.43	-0.96	-2.39		
	6.52	-1.41	-0.54	-1.95		
	8.38	-1.39	-0.21	-1.60		
	9.45	-1.38	-0.26	-1.64		
	11.77	-1.36	-0.27	-1.63		
	14.81	-1.33	-0.45	-1.78		
	17.47	-1.30	-0.81	-2.11		
	18.99	-1.28	-0.52	-1.80		
	20.51	-1.27	-1.04	-2.31		
22.45	-1.25	-0.66	-1.91			
HBF 10m	0.49	-1.47	-17.66	-19.13		
	1.10	-1.46	-8.70	-10.16		
	2.10	-1.45	-5.72	-7.17		
	4.15	-1.43	-4.76	-6.19		
	7.92	-1.39	-3.20	-4.59		
	9.45	-1.38	-2.34	-3.72		
	11.37	-1.36	-1.90	-3.26		
	12.95	-1.34	-1.53	-2.87		
	15.09	-1.32	-1.65	-2.97		
	17.50	-1.30	-1.07	-2.37		
	21.24	-1.26	-0.69	-1.95		
23.96	-1.24	-0.75	-1.99			
HBF 50m	0.43	-1.47	-15.34	-5.68		
	1.52	-1.46	-16.24	-5.68		
	1.98	-1.45	-9.71	-5.68		
	3.51	-1.44	-7.62	-5.68		
	5.03	-1.42	-7.94	-5.68		
	6.10	-1.41	-6.93	-5.68		
	7.62	-1.40	-4.96	-5.68		
	9.08	-1.38	-4.41	-5.68		
9.88	-1.37	-5.82	-5.68			
EFF 35 0m	0.23	2.11	-2.28	-0.17	0.29	0.00
	0.53	2.10	-0.58	1.53	0.59	0.00
	0.84	2.10	-0.93	1.17	0.90	0.00
	1.20	2.10	-0.35	1.75	1.26	0.00
	1.51	2.09	-0.37	1.72	1.57	0.00
	1.81	2.09	-0.35	1.74	1.87	0.00
	2.12	2.09	-0.31	1.78	2.18	0.00
	2.52	2.08	-0.33	1.75	2.58	0.00
	2.76	2.08	-0.30	1.78	2.82	0.00
	3.06	2.08	-0.30	1.78	3.12	0.00
	3.37	2.07	-0.31	1.76	3.43	0.00
	3.67	2.07	-0.31	1.76	3.73	0.00
	4.04	2.07	-0.38	1.69	4.10	0.00
	4.31	2.07	-0.36	1.70	4.37	0.00
	4.62	2.06	-0.41	1.66	4.68	0.00
	4.89	2.06	-0.38	1.68	4.95	0.00
	5.35	2.06	-0.45	1.60	5.41	0.00
	5.87	2.05	-0.61	1.44	5.93	-0.03
	6.17	2.05	-0.33	1.72	6.23	0.00
	6.48	2.04	-0.40	1.64	6.54	0.00
7.03	2.04	-0.88	1.16	7.03	0.00	
7.70	2.03	-0.64	1.39	7.09	0.00	
8.15	2.03	-0.62	1.40	7.76	0.00	
8.67	2.02	-0.54	1.48	8.15	0.00	
9.10	2.02	-0.81	1.21	8.21	-0.02	
9.71	2.01	-1.60	0.41	8.67	-0.02	
10.30	2.01	-1.90	0.10	9.10	-0.12	
10.70	2.00	-2.72	-0.72	9.68	0.00	

Table 2. Gravitational water content, chloride concentrations, water flux, water velocity, age, cumulative chloride, and cumulative water content of soil samples.

Borehole number	Depth (m)	Gravitational potential (MPa)	Water potential (MPa)	Total potential (MPa)	Depth (m)	Osmotic potential (MPa)
	11.30	2.00	-2.44	-0.45	11.32	-0.66
	11.80	1.99	-2.84	-0.85	14.31	-0.64
	12.20	1.99	-4.11	-2.12	17.42	-0.63
	12.80	1.98	-5.04	-3.06	20.47	-0.66
	13.30	1.98	-4.80	-2.82		
	14.20	1.97	-4.58	-2.62		
	15.80	1.95	-4.65	-2.70		
	16.50	1.95	-5.00	-3.05		
	14.90	1.96	-5.41	-3.45		
	17.40	1.94	-4.89	-2.95		
	18.00	1.93	-4.89	-2.95		
	18.90	1.92	-4.54	-2.62		
	19.40	1.92	-4.68	-2.76		
	20.40	1.91	-4.32	-2.41		
	0.23	2.11	-11.50	-9.42	0.59	-1.00
	0.53	2.10	-9.79	-7.68	1.05	-0.95
	0.99	2.10	-9.52	-7.42	1.36	-0.84
	1.30	2.10	-7.77	-5.68	1.66	-0.79
	1.60	2.09	-6.92	-4.82	1.97	-0.88
	1.91	2.09	-7.69	-5.60	2.27	-0.85
	2.21	2.09	-6.22	-4.13	2.58	-0.85
	2.85	2.08	-7.41	-5.33	3.22	-0.78
	3.15	2.08	-7.16	-5.09	3.52	-0.74
	3.46	2.07	-7.14	-5.07	3.83	-0.61
	3.76	2.07	-7.79	-5.72	4.13	-0.74
	4.07	2.07	-8.90	-6.84	4.47	-0.42
	4.40	2.06	-7.49	-5.42	4.77	-0.73
	4.71	2.06	-7.78	-5.72	5.07	-0.64
	5.01	2.06	-7.65	-5.59	5.47	-0.68
	5.96	2.05	-8.41	-6.36	6.32	-0.65
	6.26	2.05	-7.82	-5.77	6.63	-0.64
	6.57	2.04	-6.56	-4.52	8.21	-0.61
	6.87	2.04	-6.73	-4.68	9.86	-0.60
	7.24	2.04	-6.66	-4.62	11.30	-0.43
	7.64	2.03	-6.61	-4.58	12.80	-0.63
	8.15	2.03	-6.35	-4.33	14.50	-0.71
	8.61	2.02	-6.18	-4.16	16.10	-0.63
	9.19	2.02	-6.95	-4.93	17.60	-0.67
	9.80	2.01	-7.74	-5.73	20.90	-0.67
	10.30	2.01	-6.69	-4.68	23.80	-0.69
	10.70	2.00	-6.35	-4.35	26.90	-0.66
	11.20	2.00	-6.26	-4.26	30.00	-0.75
	11.90	1.99	-5.81	-3.81		
	12.30	1.99	-6.06	-4.07		
	12.80	1.98	-6.08	-4.10		
EFF 36 10m	13.20	1.98	-5.83	-3.85		
	13.70	1.97	-5.81	-3.83		
	14.50	1.97	-5.76	-3.79		
	15.40	1.96	-5.74	-3.79		
	16.00	1.95	-5.70	-3.75		
	17.00	1.94	-5.59	-3.64		
	17.60	1.94	-5.74	-3.81		
	18.50	1.93	-5.18	-3.25		
	19.10	1.92	-5.40	-3.48		
	19.90	1.91	-5.41	-3.49		
	20.80	1.90	-4.90	-2.99		
	22.10	1.89	-5.52	-3.63		
	23.50	1.88	-5.12	-3.24		
	25.30	1.86	-4.90	-3.04		
	26.80	1.85	-4.88	-3.03		
	29.90	1.81	-5.27	-3.46		
	0.27	2.11	-4.87	-2.77	0.22	-0.33
	0.57	2.10	-7.15	-5.05	0.53	-0.89

Table 2. Gravitational water content, chloride concentrations, water flux, water velocity, age, cumulative chloride, and cumulative water content of soil samples.

Borehole number	Depth (m)	Gravitational potential (MPa)	Water potential (MPa)	Total potential (MPa)	Depth (m)	Osmotic potential (MPa)
EFF 59 10m	1.33	2.09	-6.89	-4.79	1.29	-1.01
	1.61	2.09	-7.76	-5.67	1.56	-0.93
	1.94	2.09	-6.68	-4.60	1.90	-0.93
	2.25	2.09	-7.88	-5.79	2.20	-0.92
	2.89	2.08	-6.13	-4.05	2.84	-0.86
	3.19	2.08	-6.15	-4.08	3.15	-0.82
	3.50	2.07	-6.90	-4.82	3.45	-0.80
	3.80	2.07	-6.51	-4.44	3.76	-0.83
	4.12	2.07	-9.41	-7.34	4.06	-0.81
	4.63	2.06	-7.01	-4.95	4.58	-0.56
	4.93	2.06	-6.86	-4.80	4.88	-0.74
	5.24	2.06	-5.82	-3.76	5.19	-0.73
	6.00	2.05	-5.58	-3.53	5.95	-0.65
	6.30	2.05	-6.11	-4.07	6.26	-0.65
	6.61	2.04	-6.16	-4.11	6.56	-0.63
	6.91	2.04	-5.74	-3.70	6.87	-0.64
	7.17	2.04	-7.65	-5.61	6.96	-0.66
	7.55	2.03	-5.70	-3.66	7.51	-0.62
	7.95	2.03	-5.72	-3.69	7.90	-0.65
	8.25	2.03	-6.11	-4.08	8.21	-0.67
	9.81	2.01	-5.67	-3.65	9.76	-0.65
	11.20	2.00	-5.57	-3.57	11.10	-0.68
	11.90	1.99	-5.93	-3.94	11.80	-0.74
	12.70	1.98	-5.47	-3.49	12.70	-0.70
	14.30	1.97	-5.35	-3.38	14.20	-0.70
	15.80	1.95	-5.47	-3.52	15.80	-0.42
17.40	1.94	-4.91	-2.97	17.40	-1.11	
19.00	1.92	-5.18	-3.26	18.90	-0.70	
20.50	1.91	-4.86	-2.95	20.50	-0.74	
22.10	1.89	-5.08	-3.19	22.00	-0.69	
23.60	1.88	-4.93	-3.06	23.60	-0.73	
25.30	1.86	-4.93	-3.07	25.20	-0.71	
				26.70	-0.70	
EFF 88 0m	0.27	2.11	-3.03	-0.92	0.22	-0.02
	0.57	2.10	-2.90	-0.80	0.53	0.00
	1.15	2.10	-2.00	0.10	1.10	0.00
	1.46	2.09	-1.30	0.80	1.41	0.00
	1.76	2.09	-0.80	1.29	1.71	0.00
	2.07	2.09	-0.73	1.35	2.02	0.00
	2.39	2.08	-0.75	1.33	2.34	-0.04
	2.71	2.08	-0.64	1.45	2.66	-0.09
	3.01	2.08	-0.63	1.45	2.96	-0.06
	3.32	2.08	-0.63	1.44	3.57	-0.10
	3.62	2.07	-0.75	1.32	3.89	-0.09
	3.92	2.07	-1.11	0.96	4.21	-0.10
	4.26	2.07	-0.85	1.21	4.52	-0.07
	4.56	2.06	-0.62	1.45	4.82	-0.03
	4.87	2.06	-0.40	1.66	5.13	0.00
	5.17	2.06	-0.54	1.52	5.77	-0.08
	5.81	2.05	-0.59	1.47	6.29	-0.28
	6.33	2.05	-1.23	0.82	7.06	-0.32
	7.05	2.04	-1.84	0.20	7.84	-0.53
	7.89	2.03	-1.61	0.43	8.59	-0.54
8.63	2.02	-2.79	-0.77	9.15	-0.49	
9.20	2.02	-3.32	-1.30	9.73	-0.49	
9.78	2.01	-3.06	-1.05	10.90	-0.53	
10.70	2.00	-2.86	-0.85	11.70	-0.60	
11.70	1.99	-3.74	-1.75	12.50	-0.54	
12.60	1.98	-3.79	-1.81			
	0.27	2.11	-11.85	-9.75	0.03	-0.12
	0.59	2.10	-10.50	-8.39	0.46	0.00
	1.35	2.09	-5.94	-3.85	0.79	-0.01
	1.96	2.09	-1.65	0.44	1.10	-0.08

Table 2. Gravitational water content, chloride concentrations, water flux, water velocity, age, cumulative chloride, and cumulative water content of soil samples.

Borehole number	Depth (m)	Gravitational potential (MPa)	Water potential (MPa)	Total potential (MPa)	Depth (m)	Osmotic potential (MPa)
EFF 92 0m	3.18	2.08	-2.17	-0.09	1.40	-0.19
	4.40	2.06	-1.15	0.91	1.71	-0.20
	5.92	2.05	-1.02	1.03	2.01	-0.23
	6.53	2.04	-1.55	0.50	2.32	-0.24
	7.38	2.04	-1.75	0.28	2.62	-0.28
	9.21	2.02	-2.29	-0.27	2.93	-0.26
	10.43	2.01	-2.66	-0.66	3.23	-0.26
	11.65	1.99	-3.41	-1.42	3.54	-0.22
	12.87	1.98	-3.89	-1.90	3.97	-0.13
	14.03	1.97	-3.86	-1.89	4.27	-0.12
	14.75	1.96	-3.89	-1.92	4.58	-0.05
	15.96	1.95	-3.82	-1.87	4.88	-0.09
					5.36	-0.14
					5.49	-0.14
					5.67	-0.17
					5.80	-0.19
					6.10	-0.22
					6.41	-0.25
					6.71	-0.31
					7.44	-0.41
					7.87	-0.45
				8.35	-0.50	
				8.96	-0.51	
				9.57	-0.48	
				10.18	-0.48	
				10.61	-0.52	
				11.09	-0.50	
				11.53	-0.53	
				12.01	-0.54	
				12.44	-0.54	
				12.92	-0.57	
				13.78	-0.55	
				14.21	-0.56	
				14.51	-0.57	
				15.00	-0.55	
				15.42	-0.55	
				16.48	-0.54	
				17.40	-0.55	
				18.46	-0.58	
				19.38	-0.58	
				20.44	-0.62	
				21.36	-0.61	
EFF 96 10m	0.15	2.11	-27.43	-25.32	0.26	-0.01
	0.76	2.10	-13.34	-11.24	0.64	-0.54
	1.62	2.09	-8.53	-6.44	1.11	-0.77
	2.41	2.08	-7.73	-5.65	1.72	-0.83
	3.54	2.07	-8.18	-6.10	2.33	-0.75
	5.12	2.06	-7.23	-5.17	2.64	-0.76
	6.65	2.04	-6.31	-4.27	3.25	-0.71
	8.05	2.03	-6.33	-4.30	3.63	-0.70
	9.69	2.01	-5.75	-3.73	4.18	-0.68
	11.13	2.00	-6.69	-4.69	4.79	-0.63
	12.50	1.99	-5.75	-3.77	5.23	-0.61
	14.02	1.97	-5.17	-3.20	5.64	-0.61
	15.55	1.96	-5.66	-3.71	6.54	-0.58
	16.89	1.94	-5.20	-3.25	7.21	-0.59
					7.79	-0.56
					8.34	-0.57
				8.75	-0.55	
				9.19	-0.60	
				10.21	-0.60	
				10.84	-0.56	
				11.22	-0.60	

Table 2. Gravitational water content, chloride concentrations, water flux, water velocity, age, cumulative chloride, and cumulative water content of soil samples.

Borehole number	Depth (m)	Gravitational potential (MPa)	Water potential (MPa)	Total potential (MPa)	Depth (m)	Osmotic potential (MPa)
					12.41	-0.60
					13.32	-0.61
					14.11	-0.62
					15.45	-0.62
					16.25	-0.61
					16.67	-0.62
RLB 0m	0.15	-1.05	-0.33	-1.38	0.03	0.00
	0.37	-1.05	-6.70	-7.75	0.47	0.00
	0.91	-1.04	-5.12	-6.16	1.02	-0.01
	2.47	-1.02	-2.56	-3.58	1.46	-0.01
	4.02	-1.01	-4.65	-5.66	2.58	0.00
	5.76	-0.99	-3.39	-4.38	3.19	-0.01
	7.41	-0.98	-2.19	-3.17	4.13	0.00
	9.63	-0.95	-2.47	-3.42	4.51	-0.02
	10.85	-0.94	-2.01	-2.95	4.95	-0.11
	12.92	-0.92	-1.97	-2.89	5.43	-0.10
	14.36	-0.91	-1.82	-2.73	6.04	-0.02
	15.21	-0.90	-1.69	-2.59	7.07	0.00
	17.47	-0.88	-1.81	-2.69	7.51	0.00
	19.05	-0.86	-1.71	-2.57	8.15	0.00
	20.45	-0.85	-1.60	-2.45	9.08	0.00
					10.23	-0.01
					10.94	0.00
					12.10	0.00
					13.01	0.00
					14.01	0.00
				16.03	0.00	
				18.20	0.00	
				20.10	-0.01	
RLB 50m	0.67	-1.04	-7.17		0.03	-0.98
	1.68	-1.03	-7.02		0.32	-0.05
	3.29	-1.02	-5.36		0.59	0.00
	4.48	-1.01	-5.91		0.76	-0.38
	6.25	-0.99	-5.19		1.23	-0.36
	7.53	-0.98	-4.77		1.60	-0.26
					2.06	-0.31
					2.48	-0.28
					3.22	-0.30
					4.13	-0.27
					4.57	-0.30
					5.14	-0.24
					6.17	-0.20
					7.07	-0.19
				8.18	-0.15	
RFF 0m	0.37	0.83	-5.86		0.03	0.00
	1.31	0.82	-3.37		0.43	-0.01
	2.10	0.81	-2.13		0.98	0.00
	3.23	0.80	-1.72		1.37	0.00
	4.82	0.79	-1.07		1.77	0.00
	5.82	0.78	-1.00		2.16	0.00
	7.35	0.76	-1.08		2.50	0.00
	8.93	0.75	-0.47		2.90	0.00
	10.39	0.73	-0.50		3.29	0.00
	11.92	0.72	-0.27		4.08	-0.01
	13.53	0.70	-0.31		5.04	-0.03
	15.03	0.69	-0.26		6.05	-0.04
	16.95	0.67	-1.15		7.06	-0.02
	18.47	0.65	-1.24		8.20	-0.03
	19.99	0.64	-1.24		9.10	-0.03
	21.21	0.63	-1.11		10.10	-0.03
23.04	0.61	-0.98		11.02	-0.03	
24.96	0.59	-1.39		12.15	-0.04	
				13.17	-0.03	

Table 2. Gravitational water content, chloride concentrations, water flux, water velocity, age, cumulative chloride, and cumulative water content of soil samples.

Borehole number	Depth (m)	Gravitational potential (MPa)	Water potential (MPa)	Total potential (MPa)	Depth (m)	Osmotic potential (MPa)
					14.16	-0.02
					16.05	-0.01
					17.01	0.00
					18.14	0.00
					19.10	0.00
					20.06	0.00
					20.85	0.00
					21.67	0.00
					23.10	-0.01
					24.63	0.00
RFF 10m	0.37	0.83	-10.39		0.03	0.00
	0.76	0.83	-8.33		0.43	-0.05
	1.62	0.82	-5.18		0.82	-0.28
	2.41	0.81	-4.07		1.28	-0.38
	3.75	0.80	-3.29		1.68	-0.23
	4.94	0.78	-3.10		2.07	-0.15
	6.46	0.77	-3.09		2.47	-0.13
	7.86	0.76	-2.76		3.02	-0.11
	9.24	0.74	-2.34		3.41	-0.10
	10.39	0.73	-2.20		3.98	-0.09
	11.92	0.72	-2.04		5.17	-0.07
	13.44	0.70	-1.88		6.13	-0.06
	15.15	0.68	-1.84		7.10	-0.06
	16.34	0.67	-2.01		8.09	-0.05
					9.07	-0.04
				10.09	-0.03	
				11.02	-0.03	
				12.15	-0.03	
				14.07	-0.01	
				16.00	0.00	
RFF 50m	0.15	-0.83	-4.12	-4.95	0.03	0.00
	0.76	-0.83	-9.36	-10.19	0.47	-0.01
	1.22	-0.82	-3.43	-4.25	0.87	-0.04
	1.62	-0.82	-4.30	-5.12	1.33	-0.09
	2.44	-0.81	-3.06	-3.87	1.71	-0.10
	2.91	-0.80	-3.13	-3.93	2.15	-0.10
	3.49	-0.80	-2.73	-3.53	2.56	-0.09
	4.07	-0.79	-2.77	-3.56	3.00	-0.09
	4.62	-0.79	-2.58	-3.37	3.58	-0.09
	5.41	-0.78	-2.57	-3.35	4.16	-0.07
	6.51	-0.77	-2.23	-3.00	4.53	-0.07
	7.03	-0.76	-2.42	-3.18	5.11	-0.06
	8.03	-0.75	-2.21	-2.96	6.05	-0.06
	9.01	-0.75	-2.11	-2.86	6.96	-0.06
	10.10	-0.73	-2.34	-3.07	7.94	-0.05
11.45	-0.72	-2.09	-2.81	8.92	-0.04	
13.14	-0.70	-2.53	-3.23	10.01	-0.04	
				10.99	-0.04	
				11.96	-0.03	
				13.06	-0.03	

Table 3. Gravimetric water content, chloride concentrations, water flux, water velocity, age, cumulative chloride, and cumulative water content of soil samples.*

Well number	Depth (m)	Interval thickness (m)	Gravimetric water content (g/g)	Chloride (mg Cl/kg soil)	Chloride (g Cl m-3 water)	Water flux (mm/yr)	Water velocity (mm/yr)	Age (yr)	Cumulative Cl (g m-2)	Cumulative H2O (m)
HBF 0m	0.03	0.03	0.035	3.3	94.0				0.15	0.00
	1.30	1.26	0.046	1.6	34.6				3.18	0.09
	2.82	1.52	0.032	1.8	55.3				7.19	0.16
	3.28	0.46	0.031	0.8	24.4				7.70	0.18
	4.60	1.33	0.045	0.6	12.6				8.84	0.27
	6.13	1.52	0.106	1.9	17.5				13.09	0.52
	7.19	1.07	0.049	0.9	17.5				14.45	0.59
	8.05	0.85	0.145	1.1	7.9				15.92	0.78
	9.11	1.07	0.089	0.3	3.7				16.45	0.92
	10.07	0.96	0.101	0.5	4.5				17.10	1.07
	11.03	0.96	0.166	0.4	2.6				17.73	1.31
	12.16	1.13	0.125	0.5	3.9				18.54	1.52
	13.12	0.96	0.140	0.4	3.1				19.16	1.72
	14.08	0.96	0.132	0.3	2.5				19.64	1.91
	15.21	1.13	0.172	24.1	140.3				60.37	2.20
	16.17	0.96	0.166	53.0	320.0				136.72	2.44
17.13	0.96	0.172	90.0	522.8				266.38	2.69	
19.05	1.92	0.153	147.2	959.2				690.42	3.13	
21.08	2.03	0.142	184.9	1300.0				1252.53	3.56	
23.23	2.15	0.168	145.9	866.8				1722.75	4.10	
HBF 10m	0.03	0.03	0.033	5.4	167.0				0.25	0.00
	0.55	0.52	0.065	2.6	39.4				2.25	0.05
	1.16	0.61	0.044	2.2	48.7				4.23	0.09
	1.65	0.49	0.015	0.7	46.0				4.73	0.10
	2.62	0.98	0.010	0.8	80.8				5.92	0.12
	3.14	0.52	0.114	1.1	9.7				6.78	0.21
	3.53	0.39	0.057	1.4	24.8				7.60	0.24
	4.21	0.68	0.061	1.0	16.6				8.63	0.30
	4.72	0.52	0.013	0.8	62.4				9.26	0.31
	5.17	0.44	0.011	2.4	221.5				10.83	0.32
	5.67	0.50	0.014	0.6	46.9				11.32	0.33
	6.19	0.52	0.014	0.9	64.2				12.02	0.34
	6.45	0.26	0.017	1.3	74.4				12.51	0.35
	7.19	0.75	0.092	0.5	5.4				13.07	0.45
	7.59	0.40	0.093	0.4	4.5				13.32	0.51
	8.15	0.56	0.129	0.5	4.3				13.78	0.61

Table 3. Gravimetric water content, chloride concentrations, water flux, water velocity, age, cumulative chloride, and cumulative water content of soil samples.*

Well number	Depth (m)	Interval thickness (m)	Gravimetric water content (g/g)	Chloride (mg Cl/kg soil)	Chloride (g Cl m-3 water)	Water flux (mm/yr)	Water velocity (mm/yr)	Age (yr)	Cumulative Cl (g m-2)	Cumulative H2O (m)
	9.11	0.96	0.078	0.5	6.5				14.52	0.73
	10.07	0.96	0.062	0.5	7.8				15.21	0.82
	11.03	0.96	0.105	0.3	2.9				15.64	0.97
	11.99	0.96	0.081	2.8	34.1				19.62	1.08
	13.01	1.02	0.070	18.2	259.7				47.42	1.19
	14.14	1.13	0.101	109.5	1084.9				232.58	1.36
	15.15	1.01	0.143	255.8	1791.9				618.52	1.58
	16.11	0.96	0.155	269.3	1738.5				1006.41	1.80
	17.13	1.02	0.171	219.4	1281.1				1342.50	2.06
	18.03	0.90	0.121	148.4	1229.8				1542.62	2.22
	18.82	0.79	0.155	166.8	1077.5				1740.94	2.41
	19.05	0.23	0.153	154.5	1009.7				1793.92	2.46
	20.18	1.13	0.145	148.6	1023.1				2045.33	2.71
	21.08	0.90	0.137	167.7	1225.8				2271.53	2.89
	22.10	1.02	0.160	219.7	1370.0				2607.99	3.14
	23.23	1.13	0.161	128.6	800.8				2825.53	3.41
	24.19	0.96	0.065	62.1	955.6				2914.97	3.50
	25.10	0.91	0.053	12.5	236.9				2932.13	3.57
	26.14	1.04	0.037	5.7	152.3				2940.98	3.63
	0.03	0.03	0.035	2.0	58.0	1.31	24.71	1	0.09	0.00
	0.49	0.46	0.057	0.7	12.0	6.30	73.06	7	0.57	0.04
	1.13	0.64	0.030	4.5	149.4	0.51	11.20	65	4.89	0.07
	1.58	0.46	0.036	23.5	647.6	0.12	2.15	277	20.99	0.09
	2.04	0.46	0.016	28.1	1775.3	0.04	1.79	532	40.28	0.11
	2.65	0.61	0.016	87.5	5359.9	0.01	0.58	1589	120.27	0.12
	3.11	0.46	0.010	51.8	5436.9	0.01	0.97	2058	155.80	0.13
HBF 50m	4.18	1.07	0.069	162.4	2363.8	0.03	0.31	5491	415.66	0.24
	4.63	0.46	0.075	184.3	2473.3	0.03	0.27	7161	542.06	0.29
	5.29	0.66	0.070	112.2	1609.7	0.05	0.45	8618	652.38	0.36
	5.70	0.41	0.043	66.6	1564.9	0.05	0.76	9161	693.47	0.38
	6.16	0.46	0.049	57.3	1162.7	0.07	0.88	9680	732.76	0.42
	6.74	0.58	0.021	24.1	1127.6	0.07	2.10	9956	753.68	0.44
	7.22	0.49	0.015	14.1	969.2	0.08	3.59	10092	763.97	0.45
	7.68	0.46	0.109	110.4	1010.9	0.07	0.46	11092	839.69	0.52
	8.24	0.56	0.107	102.5	954.5	0.08	0.49	12237	926.36	0.61
	9.31	1.07	0.092	84.3	917.5	0.08	0.60	14019	1061.27	0.76

Table 3. Gravimetric water content, chloride concentrations, water flux, water velocity, age, cumulative chloride, and cumulative water content of soil samples.*

Well number	Depth (m)	Interval thickness (m)	Gravimetric water content (g/g)	Chloride (mg Cl/kg soil)	Chloride (g Cl m-3 water)	Water flux (mm/yr)	Water velocity (mm/yr)	Age (yr)	Cumulative Cl (g m-2)	Cumulative H2O (m)
	0.29	0.29	0.096	BD2	BD2					0.05
	0.59	0.30	0.106	BD2	BD2					0.11
	0.90	0.30	0.107	BD2	BD2					0.16
	1.26	0.37	0.120	BD2	BD2					0.24
	1.57	0.30	0.149	BD2	BD2					0.32
	1.87	0.30	0.188	BD2	BD2					0.42
	2.18	0.30	0.158	BD2	BD2					0.50
	2.58	0.40	0.171	BD2	BD2					0.62
	2.82	0.24	0.162	BD2	BD2					0.69
	3.12	0.30	0.148	BD2	BD2					0.77
	3.43	0.30	0.197	BD2	BD2					0.88
	3.73	0.30	0.155	BD2	BD2					0.96
	4.10	0.37	0.144	BD2	BD2					1.05
	4.37	0.27	0.135	BD2	BD2					1.11
	4.68	0.30	0.133	BD2	BD2					1.19
	4.95	0.27	0.072	BD2	BD2					1.22
	5.41	0.46	0.042	BD2	BD2					1.25
	5.93	0.52	0.110	21.6	196.4					1.35
	6.23	0.30	0.120	BD2	BD2					1.42
	6.54	0.30	0.193	BD2	BD2					1.52
	7.03	0.49	0.162	3.0	18.6					1.66
	7.09	0.06	0.155	BD2	BD2					1.68
	7.70	0.61	0.130	9.9	75.7					1.81
	7.76	0.06	0.153	BD2	BD2					1.83
	8.15	0.40	0.132	3.0	22.7					1.92
	8.21	0.06	0.157	18.0	114.7					1.94
	8.67	0.46	0.122	19.4	158.4					2.04
EFF 35 0m	8.73	0.06	0.127							2.05
	9.10	0.37	0.132	118.1	892.9					2.14
	9.16	0.06	0.131							2.15
	9.68	0.52	0.187	BD2	BD2					2.32
	9.71	0.03	0.197	568.8	2882.3					2.33
	10.32	0.61	0.084							2.42
	10.71	0.40	0.212							2.57
	11.32	0.61	0.152	790.1	5205.3					2.73
	11.84	0.52	0.158							2.87

Table 3. Gravimetric water content, chloride concentrations, water flux, water velocity, age, cumulative chloride, and cumulative water content of soil samples.*

Well number	Depth (m)	Interval thickness (m)	Gravimetric water content (g/g)	Chloride (mg Cl/kg soil)	Chloride (g Cl m-3 water)	Water flux (mm/yr)	Water velocity (mm/yr)	Age (yr)	Cumulative Cl (g m-2)	Cumulative H2O (m)
	12.27	0.43	0.122							2.96
	12.88	0.61	0.084							3.05
	13.40	0.52	0.094							3.14
	14.31	0.91	0.155	784.6	5076.4					3.38
	14.95	0.64	0.150							3.55
	15.86	0.91	0.171							3.83
	16.54	0.67	0.141							3.99
	17.42	0.88	0.132	651.8	4945.4					4.19
	18.09	0.67	0.129							4.35
	18.91	0.82	0.169							4.59
	19.46	0.55	0.166							4.75
	20.47	1.01	0.157	823.9	5255.0					5.02
	0.59	0.59	0.045	358.9	7915.6	0.01	0.12	4931	373.31	0.05
	1.05	0.46	0.056	428.3	7582.7	0.01	0.10	9459	716.01	0.09
	1.36	0.30	0.099	657.7	6670.1	0.01	0.07	14093	1066.82	0.14
	1.66	0.30	0.125	780.4	6243.8	0.01	0.06	19592	1483.08	0.21
	1.97	0.30	0.124	859.6	6954.6	0.01	0.05	25649	1941.61	0.28
	2.27	0.30	0.104	704.6	6748.7	0.01	0.06	30613	2317.42	0.33
	2.58	0.30	0.082	554.0	6733.1	0.01	0.08	34517	2612.91	0.38
	2.91	0.34	0.093	604.6	6473.7	0.01	0.07	39203	2967.68	0.43
	3.22	0.30	0.086	532.5	6197.5	0.01	0.08	42956	3251.74	0.48
	3.52	0.30	0.113	663.4	5875.9	0.01	0.07	47630	3605.58	0.54
	3.83	0.30	0.090	437.0	4860.9	0.02	0.10	50709	3838.66	0.59
	4.13	0.30	0.086	509.9	5905.9	0.01	0.08	54301	4110.62	0.63
	4.47	0.34	0.085	283.9	3330.9	0.02	0.15	56502	4277.20	0.68
	4.77	0.30	0.052	303.3	5782.8	0.01	0.14	58639	4438.97	0.71
EFF 36 10m	5.07	0.30	0.047	237.5	5046.8	0.01	0.18	60312	4565.64	0.74
	5.47	0.40	0.039	212.0	5383.9	0.01	0.20	62254	4712.64	0.76
	6.02	0.55	0.072	360.2	5012.0	0.02	0.12	66823	5058.49	0.83
	6.32	0.30	0.056	287.2	5119.7	0.01	0.15	68847	5211.71	0.86
	6.63	0.30	0.110	560.7	5083.4	0.01	0.08	72798	5510.77	0.92
	8.21	1.58	0.090	435.4	4840.2	0.02	0.10	88752	6718.53	1.17
	9.86	1.65	0.109	518.9	4745.8	0.02	0.08	108495	8213.08	1.48
	11.29	1.43	0.193	655.6	3405.4	0.02	0.07	130208	9856.75	1.97
	12.85	1.55	0.074	370.5	4996.1	0.02	0.12	143521	10864.56	2.17
	14.52	1.68	0.131	744.2	5663.2	0.01	0.06	172361	13047.75	2.55

Table 3. Gravimetric water content, chloride concentrations, water flux, water velocity, age, cumulative chloride, and cumulative water content of soil samples.*

Well number	Depth (m)	Interval thickness (m)	Gravimetric water content (g/g)	Chloride (mg Cl/kg soil)	Chloride (g Cl m-3 water)	Water flux (mm/yr)	Water velocity (mm/yr)	Age (yr)	Cumulative Cl (g m-2)	Cumulative H2O (m)
	16.08	1.55	0.158	784.0	4967.3	0.02	0.06	200536	15180.57	2.98
	17.63	1.55	0.137	730.6	5314.0	0.01	0.06	226790	17168.03	3.36
	20.86	3.23	0.165	879.5	5335.4	0.01	0.05	292482	22140.89	4.29
	23.76	2.90	0.171	932.1	5448.3	0.01	0.05	354877	26864.21	5.16
	26.87	3.11	0.152	799.5	5263.9	0.01	0.05	412340	31214.11	5.98
	29.98	3.11	0.168	998.7	5946.3	0.01	0.04	484119	36647.79	6.90
	0.22	0.22	0.107	278.6	2593.2	0.03	0.16	1423	107.75	0.04
	0.53	0.30	0.088	623.5	7062.3	0.01	0.07	5817	440.31	0.09
	0.92	0.40	0.073	610.6	8396.2	0.01	0.07	11410	863.74	0.14
	1.29	0.37	0.073	590.2	8054.2	0.01	0.07	16400	1241.51	0.19
	1.56	0.27	0.042	309.7	7365.5	0.01	0.14	18364	1390.17	0.21
	1.90	0.34	0.105	779.9	7432.8	0.01	0.06	24409	1847.76	0.27
	2.20	0.30	0.094	688.8	7342.0	0.01	0.06	29263	2215.19	0.32
	2.60	0.40	0.086	643.9	7506.6	0.01	0.07	35161	2661.70	0.38
	2.84	0.24	0.093	633.0	6814.5	0.01	0.07	38729	2931.80	0.42
	3.15	0.30	0.093	601.7	6489.4	0.01	0.07	42969	3252.76	0.47
	3.45	0.30	0.088	562.1	6371.1	0.01	0.08	46930	3552.57	0.51
	3.76	0.30	0.088	579.7	6570.7	0.01	0.07	51015	3861.80	0.56
	4.06	0.31	0.076	485.3	6417.8	0.01	0.09	54468	4123.23	0.60
	4.58	0.52	0.085	374.6	4429.5	0.02	0.12	58929	4460.94	0.68
	4.88	0.30	0.063	369.7	5848.3	0.01	0.12	61534	4658.11	0.71
	5.19	0.30	0.041	235.6	5748.2	0.01	0.18	63194	4783.79	0.73
	5.95	0.76	0.034	173.7	5138.1	0.01	0.25	66255	5015.47	0.78
	6.26	0.30	0.137	703.5	5125.4	0.01	0.06	71211	5390.70	0.85
	6.56	0.30	0.109	544.0	5013.8	0.02	0.08	75045	5680.90	0.91
	6.87	0.30	0.131	657.8	5037.7	0.02	0.07	79680	6031.74	0.98
	6.96	0.09	0.103	534.7	5215.1	0.01	0.08	80810	6117.30	1.00
	7.51	0.55	0.104	509.6	4905.6	0.02	0.08	87273	6606.60	1.09
EFF 59 10m	7.90	0.40	0.093	479.2	5169.3	0.01	0.09	91663	6938.87	1.16
	8.21	0.30	0.071	375.4	5265.9	0.01	0.12	94308	7139.09	1.20
	9.76	1.55	0.124	644.7	5181.6	0.01	0.07	117474	8892.81	1.54
	11.13	1.37	0.159	851.1	5368.2	0.01	0.05	144461	10935.71	1.92
	11.83	0.70	0.124	727.4	5873.7	0.01	0.06	156249	11828.07	2.07
	12.69	0.85	0.121	674.0	5567.8	0.01	0.06	169547	12834.74	2.25
	14.24	1.55	0.139	765.9	5509.6	0.01	0.06	197071	14918.30	2.63
	15.80	1.55	0.153	501.2	3285.7	0.02	0.09	215083	16281.76	3.04

Table 3. Gravimetric water content, chloride concentrations, water flux, water velocity, age, cumulative chloride, and cumulative water content of soil samples.*

Well number	Depth (m)	Interval thickness (m)	Gravimetric water content (g/g)	Chloride (mg Cl/kg soil)	Chloride (g Cl m-3 water)	Water flux (mm/yr)	Water velocity (mm/yr)	Age (yr)	Cumulative Cl (g m-2)	Cumulative H2O (m)
	17.35	1.55	0.093	817.3	8803.9	0.01	0.05	244454	18505.17	3.29
	18.91	1.55	0.145	799.7	5511.8	0.01	0.05	273192	20680.63	3.69
	20.46	1.55	0.168	985.7	5860.7	0.01	0.04	308613	23362.03	4.15
	22.01	1.55	0.174	952.4	5475.3	0.01	0.05	342837	25952.79	4.62
	23.57	1.55	0.150	863.6	5752.8	0.01	0.05	373872	28302.10	5.03
	25.21	1.65	0.131	739.7	5641.7	0.01	0.06	402016	30432.58	5.41
	26.68	1.46	0.134	741.6	5549.6	0.01	0.06	427098	32331.31	5.75
	0.22	0.22	0.093	15.1	162.1					0.04
	0.53	0.30	0.080	BD2	BD2					0.08
	1.10	0.58	0.090	BD2	BD2					0.17
	1.41	0.30	0.138	BD2	BD2					0.24
	1.71	0.30	0.160	BD2	BD2					0.33
	2.02	0.30	0.148	BD2	BD2					0.41
	2.34	0.32	0.139	37.0	266.7					0.49
	2.66	0.32	0.160	104.8	653.6					0.58
	2.96	0.30	0.181	79.6	438.9					0.67
	3.57	0.61	0.145	112.3	774.0					0.83
	3.89	0.32	0.116	80.7	694.6					0.89
	4.21	0.32	0.089	65.0	733.0					0.94
EFF 88 0m	4.52	0.30	0.090	47.9	532.2					0.99
	4.82	0.30	0.091	19.4	214.3					1.04
	5.13	0.30	0.044	BD2	BD2					1.06
	5.77	0.64	0.096	55.1	572.1					1.17
	6.29	0.52	0.186	401.3	2160.5					1.34
	7.06	0.78	0.105	256.5	2453.4					1.48
	7.84	0.78	0.153	636.5	4157.2					1.69
	8.59	0.75	0.143	612.6	4272.2					1.88
	9.15	0.56	0.060	231.0	3870.4					1.93
	9.73	0.58	0.159	616.5	3867.4					2.10
	10.95	1.22	0.130	544.4	4195.0					2.37
	11.65	0.70	0.129	614.9	4753.3					2.53
	12.50	0.85	0.130	552.2	4244.2					2.73
	0.03	0.03	0.050	46.9	933.2				2.86	0.00
	0.46	0.43	0.061	1.5	24.1				4.14	0.06
	0.79	0.33	0.058	4.7	80.2				7.21	0.09
	1.10	0.30	0.069	44.5	643.4				34.31	0.14

Table 3. Gravimetric water content, chloride concentrations, water flux, water velocity, age, cumulative chloride, and cumulative water content of soil samples.*

Well number	Depth (m)	Interval thickness (m)	Gravimetric water content (g/g)	Chloride (mg Cl/kg soil)	Chloride (g Cl m-3 water)	Water flux (mm/yr)	Water velocity (mm/yr)	Age (yr)	Cumulative Cl (g m-2)	Cumulative H2O (m)
	1.40	0.30	0.094	136.2	1452.4				117.37	0.19
	1.71	0.30	0.092	141.3	1535.1				203.51	0.25
	2.01	0.30	0.113	199.6	1759.2				325.21	0.32
	2.32	0.30	0.120	224.5	1872.8				462.08	0.39
	2.62	0.30	0.127	279.7	2202.5				632.59	0.47
	2.93	0.30	0.114	227.3	2002.4				771.16	0.54
	3.23	0.30	0.128	260.8	2036.1				930.16	0.62
	3.54	0.30	0.132	225.7	1710.8				1067.75	0.70
	3.97	0.43	0.089	86.1	971.7				1142.58	0.77
	4.27	0.30	0.078	74.2	949.0				1187.79	0.82
	4.58	0.30	0.086	30.2	350.3				1206.21	0.87
	4.88	0.30	0.068	46.8	687.3				1234.74	0.92
	5.36	0.48	0.062	67.6	1097.3				1299.68	0.98
	5.49	0.13	0.069	74.7	1085.1				1319.03	0.99
	5.67	0.18	0.062	80.1	1282.4				1347.10	1.01
	5.80	0.13	0.116	168.3	1453.4				1390.71	1.04
	6.10	0.30	0.173	289.0	1670.3				1566.87	1.15
	6.41	0.30	0.139	266.7	1917.5				1729.43	1.23
	6.71	0.30	0.143	345.7	2413.6				1940.16	1.32
	7.44	0.72	0.108	346.1	3192.2				2441.22	1.48
	7.87	0.43	0.166	588.1	3539.2				2952.06	1.62
	8.35	0.48	0.061	238.1	3934.8				3180.71	1.68
	8.96	0.61	0.112	458.3	4092.1				3739.51	1.82
	9.57	0.61	0.180	690.0	3824.3				4580.73	2.04
	10.18	0.61	0.078	295.6	3776.4				4941.07	2.13
	10.61	0.43	0.149	614.4	4112.9				5474.75	2.26
EFF 92 0m	11.09	0.48	0.136	539.7	3954.4				5992.91	2.39
	11.53	0.43	0.148	629.2	4261.1				6539.45	2.52
	12.01	0.48	0.137	596.9	4346.4				7112.53	2.65
	12.44	0.43	0.093	398.9	4284.5				7459.07	2.74
	12.92	0.48	0.100	456.4	4568.5				7897.30	2.83
	13.78	0.85	0.140	614.7	4400.2				8946.47	3.07
	14.21	0.43	0.154	697.5	4519.9				9552.39	3.20
	14.51	0.30	0.154	700.9	4538.1				9968.98	3.30
	15.00	0.50	0.153	674.5	4411.1				10637.13	3.45
	15.42	0.42	0.169	738.0	4366.9				11255.73	3.59

Table 3. Gravimetric water content, chloride concentrations, water flux, water velocity, age, cumulative chloride, and cumulative water content of soil samples.*

Well number	Depth (m)	Interval thickness (m)	Gravimetric water content (g/g)	Chloride (mg Cl/kg soil)	Chloride (g Cl m-3 water)	Water flux (mm/yr)	Water velocity (mm/yr)	Age (yr)	Cumulative Cl (g m-2)	Cumulative H2O (m)
	16.48	1.06	0.153	659.1	4300.8				12651.97	3.91
	17.40	0.91	0.101	439.4	4366.4				13455.62	4.10
	18.46	1.07	0.164	759.8	4643.3				15076.81	4.45
	19.38	0.91	0.161	743.6	4624.2				16436.73	4.74
	20.44	1.07	0.226	1124.8	4969.3				18836.54	5.22
	21.36	0.91	0.169	829.8	4917.4				20354.07	5.53
	0.26	0.26	0.063	3.7	58.9	1.29	10.25	25	1.91	0.03
	0.64	0.38	0.043	187.3	4327.7	0.02	0.20	1911	144.64	0.07
	1.11	0.47	0.041	260.7	6357.8	0.01	0.15	5165	390.97	0.10
	1.72	0.61	0.112	769.9	6875.2	0.01	0.05	17564	1329.61	0.24
	2.33	0.61	0.068	418.2	6176.4	0.01	0.09	24300	1839.52	0.32
	2.64	0.30	0.096	598.7	6249.7	0.01	0.06	29122	2204.51	0.38
	3.25	0.61	0.088	505.5	5760.6	0.01	0.07	37263	2820.84	0.49
	3.63	0.38	0.091	523.4	5723.6	0.01	0.07	42532	3219.64	0.56
	4.18	0.55	0.070	383.3	5508.3	0.01	0.10	48087	3640.19	0.63
	4.79	0.61	0.046	233.1	5106.7	0.01	0.16	51842	3924.45	0.69
	5.23	0.44	0.053	261.5	4891.2	0.02	0.14	54896	4155.63	0.74
	5.64	0.41	0.040	196.2	4910.7	0.02	0.19	57029	4317.10	0.77
	6.54	0.90	0.116	538.0	4654.0	0.02	0.07	69809	5284.57	0.98
	7.21	0.67	0.117	549.9	4713.9	0.02	0.07	79551	6022.05	1.13
EFF 96 10m	7.79	0.58	0.083	373.5	4475.4	0.02	0.10	85266	6454.60	1.23
	8.34	0.55	0.107	489.4	4577.8	0.02	0.08	92359	6991.61	1.35
	8.75	0.41	0.041	180.1	4398.1	0.02	0.21	94317	7139.80	1.38
	9.19	0.44	0.095	456.4	4783.1	0.02	0.08	99646	7543.19	1.47
	10.21	1.02	0.098	469.5	4784.0	0.02	0.08	112312	8501.99	1.67
	10.84	0.62	0.114	506.1	4441.0	0.02	0.07	120666	9134.43	1.81
	11.22	0.38	0.127	615.1	4825.8	0.02	0.06	126857	9603.11	1.91
	12.41	1.19	0.072	344.5	4782.8	0.02	0.11	137678	10422.22	2.08
	13.32	0.91	0.103	502.2	4887.0	0.02	0.08	149810	11340.62	2.27
	14.11	0.79	0.145	722.4	4973.3	0.02	0.05	164935	12485.59	2.50
	15.45	1.34	0.161	804.0	5001.7	0.02	0.05	193423	14642.14	2.93
	16.25	0.79	0.158	777.6	4912.7	0.02	0.05	209704	15874.61	3.18
	16.67	0.43	0.154	764.4	4960.3	0.02	0.05	218322	16527.00	3.31
	0.03	0.03	0.067	1.8	27.6				0.08	0.003
	0.47	0.44	0.044	1.3	29.7				0.96	0.033
	1.02	0.55	0.031	2.7	85.5				3.15	0.058

Table 3. Gravimetric water content, chloride concentrations, water flux, water velocity, age, cumulative chloride, and cumulative water content of soil samples.*

Well number	Depth (m)	Interval thickness (m)	Gravimetric water content (g/g)	Chloride (mg Cl/kg soil)	Chloride (g Cl m-3 water)	Water flux (mm/yr)	Water velocity (mm/yr)	Age (yr)	Cumulative Cl (g m-2)	Cumulative H2O (m)
RLB 0m	1.46	0.44	0.025	1.3	51.9				4.00	0.074
	2.58	1.11	0.038	0.9	22.6				5.44	0.138
	3.19	0.61	0.031	3.0	96.7				8.16	0.166
	4.13	0.94	0.075	1.1	14.1				9.65	0.272
	4.51	0.38	0.062	9.3	150.5				14.94	0.307
	4.95	0.44	0.047	39.4	843.9				41.04	0.338
	5.43	0.47	0.046	36.0	791.6				66.57	0.370
	6.04	0.61	0.014	2.2	156.9				68.63	0.383
	7.07	1.04	0.117	1.4	12.4				70.87	0.565
	7.51	0.44	0.081	1.3	16.4				71.75	0.618
	8.15	0.64	0.088	1.8	20.3				73.46	0.703
	9.08	0.93	0.021	0.8	36.6				74.53	0.732
	10.23	1.14	0.020	1.5	77.8				77.15	0.766
	10.94	0.72	0.082	0.9	11.3				78.15	0.854
	12.10	1.16	0.060	1.0	16.0				79.81	0.957
	13.01	0.91	0.113	0.6	5.2				80.62	1.113
	14.01	0.99	0.109	0.6	5.0				81.44	1.275
16.03	2.03	0.101	0.6	6.3				83.37	1.582	
18.20	2.16	0.106	1.8	16.5				89.06	1.926	
20.10	1.91	0.152	10.5	69.1				119.03	2.360	
RLB 50m	0.03	0.03	0.015	122.6	8348.5	0.01	0.41	74	5.61	0.00
	0.32	0.29	0.014	5.3	393.3	0.19	9.46	105	7.93	0.01
	0.59	0.27	0.050	1.3	25.9	2.92	38.91	112	8.46	0.03
	0.76	0.17	0.059	175.8	2991.1	0.03	0.29	696	52.68	0.04
	1.23	0.47	0.016	45.4	2850.3	0.03	1.11	1121	84.88	0.05
	1.60	0.37	0.015	29.2	1975.8	0.04	1.73	1333	100.88	0.06
	2.06	0.46	0.010	23.4	2417.6	0.03	2.15	1545	116.95	0.07
	2.48	0.43	0.016	35.2	2188.8	0.03	1.43	1843	139.49	0.08
	3.22	0.73	0.076	177.0	2322.5	0.03	0.29	4408	333.72	0.16
	4.13	0.91	0.077	162.3	2117.9	0.04	0.31	7349	556.33	0.27
	4.57	0.44	0.100	234.5	2345.9	0.03	0.22	9403	711.82	0.33
	5.14	0.56	0.028	52.0	1883.0	0.04	0.97	9984	755.83	0.36
	6.17	1.04	0.126	193.0	1529.0	0.05	0.26	13947	1055.81	0.55
	7.07	0.90	0.040	58.7	1481.7	0.05	0.86	14993	1134.98	0.61
	8.18	1.11	0.033	37.2	1141.1	0.07	1.36	15812	1196.98	0.66
	0.03	0.03	0.211	5.3	25.1				0.24	0.01

Table 3. Gravimetric water content, chloride concentrations, water flux, water velocity, age, cumulative chloride, and cumulative water content of soil samples.*

Well number	Depth (m)	Interval thickness (m)	Gravimetric water content (g/g)	Chloride (mg Cl/kg soil)	Chloride (g Cl m-3 water)	Water flux (mm/yr)	Water velocity (mm/yr)	Age (yr)	Cumulative Cl (g m-2)	Cumulative H2O (m)
RFF 0m	0.43	0.40	0.099	8.7	87.6				5.40	0.07
	0.98	0.55	0.073	1.2	16.4				6.38	0.13
	1.37	0.40	0.132	0.6	4.6				6.74	0.21
	1.77	0.40	0.170	0.5	2.8				7.03	0.31
	2.16	0.40	0.190	0.4	1.9				7.24	0.42
	2.50	0.34	0.206	0.3	1.3				7.38	0.52
	2.90	0.40	0.116	1.2	10.1				8.07	0.59
	3.29	0.40	0.140	3.7	26.6				10.28	0.68
	4.08	0.79	0.181	16.3	89.8				29.65	0.89
	5.04	0.96	0.180	40.8	226.9				88.37	1.15
	6.05	1.01	0.163	47.6	291.5				160.16	1.40
	7.06	1.01	0.185	33.8	182.9				211.08	1.68
	8.20	1.14	0.197	45.3	229.8				288.70	2.01
	9.10	0.90	0.172	43.5	252.4				347.33	2.25
	10.10	1.01	0.166	38.2	230.7				404.96	2.50
	11.02	0.91	0.196	42.0	214.5				462.53	2.76
	12.15	1.13	0.129	35.1	273.0				521.93	2.98
	13.17	1.02	0.128	29.6	231.4				567.27	3.18
	14.16	0.99	0.098	13.0	133.5				586.63	3.32
	16.05	1.89	0.142	7.2	50.9				607.13	3.73
17.01	0.96	0.243	8.9	36.5				619.88	4.07	
18.14	1.13	0.205	6.6	32.3				631.10	4.42	
19.10	0.96	0.203	6.6	32.5				640.61	4.71	
20.06	0.96	0.201	4.8	23.8				647.48	5.00	
20.85	0.79	0.063	1.5	24.7				649.31	5.08	
21.67	0.82	0.162	4.2	26.2				654.55	5.28	
23.10	1.43	0.040	1.5	37.9				657.85	5.37	
24.63	1.52	0.202	1.6	8.0				661.55	5.83	
RFF 10m	0.03	0.03	0.224	3.9	17.3				0.18	0.01
	0.43	0.40	0.078	31.1	399.7				18.66	0.06
	0.82	0.40	0.075	160.5	2149.8				114.07	0.10
	1.28	0.46	0.124	369.2	2980.3				367.25	0.19
	1.68	0.40	0.151	268.8	1784.3				527.05	0.28
	2.07	0.40	0.158	176.7	1115.2				632.06	0.37
	2.47	0.40	0.175	178.4	1017.4				738.09	0.47
	3.02	0.55	0.107	88.6	828.5				811.04	0.56

Table 3. Gravimetric water content, chloride concentrations, water flux, water velocity, age, cumulative chloride, and cumulative water content of soil samples.*

Well number	Depth (m)	Interval thickness (m)	Gravimetric water content (g/g)	Chloride (mg Cl/kg soil)	Chloride (g Cl m-3 water)	Water flux (mm/yr)	Water velocity (mm/yr)	Age (yr)	Cumulative Cl (g m-2)	Cumulative H2O (m)
	3.41	0.40	0.090	70.7	788.1				853.07	0.62
	3.98	0.56	0.101	69.9	688.6				912.17	0.70
	5.17	1.19	0.131	69.9	535.0				1036.79	0.93
	6.13	0.96	0.159	77.2	486.4				1147.93	1.16
	7.10	0.98	0.056	23.8	421.4				1182.71	1.24
	8.09	0.99	0.073	27.0	372.2				1222.85	1.35
	9.07	0.98	0.174	50.3	289.5				1296.43	1.61
	10.09	1.02	0.165	42.3	256.5				1361.22	1.86
	11.02	0.93	0.133	29.2	219.6				1401.93	2.04
	12.15	1.13	0.077	19.6	255.6				1435.05	2.17
	14.07	1.92	0.061	6.5	107.2				1453.75	2.35
	16.00	1.94	0.166	5.3	32.2				1469.28	2.83
	0.03	0.03	0.115	1.2	10.8	6.98	40.44	1	0.06	0.01
	0.47	0.44	0.082	5.0	60.8	1.25	10.12	44	3.36	0.06
	0.87	0.40	0.054	17.2	319.1	0.24	2.93	179	13.59	0.09
	1.33	0.46	0.155	102.3	659.3	0.11	0.49	1107	83.77	0.20
	1.71	0.38	0.172	130.2	756.8	0.10	0.39	2090	158.18	0.30
	2.15	0.44	0.166	121.6	734.3	0.10	0.41	3155	238.82	0.41
	2.56	0.41	0.174	124.6	715.4	0.11	0.40	4171	315.73	0.51
	3.00	0.44	0.084	59.3	704.4	0.11	0.85	4690	355.04	0.57
	3.58	0.58	0.083	53.6	645.6	0.12	0.94	5305	401.61	0.64
	4.16	0.58	0.156	82.9	532.9	0.14	0.61	6257	473.62	0.78
	4.53	0.37	0.179	89.9	501.9	0.15	0.56	6908	522.95	0.88
RFF 50m	5.11	0.58	0.165	77.4	468.4	0.16	0.65	7796	590.18	1.02
	6.05	0.94	0.164	74.1	452.5	0.17	0.68	9183	695.19	1.25
	6.96	0.91	0.153	64.9	425.2	0.18	0.78	10359	784.16	1.46
	7.94	0.98	0.102	36.2	356.1	0.21	1.39	11059	837.16	1.61
	8.92	0.98	0.219	71.5	326.4	0.23	0.71	12442	941.84	1.93
	10.01	1.10	0.155	45.9	296.6	0.26	1.10	13439	1017.35	2.18
	10.99	0.98	0.210	56.4	268.3	0.28	0.90	14528	1099.80	2.49
	11.96	0.98	0.098	25.1	256.0	0.30	2.01	15013	1136.48	2.63
	13.06	1.10	0.057	13.8	243.7	0.31	3.66	15313	1159.20	2.73

Table 4. Tritium and $^{36}\text{Cl}/\text{Cl}$ ratios and stable isotopes in samples collected beneath and adjacent to fissures.

Tritium			
Location	Depth (m)	Factor	Tritium units
HBF 0m	0.06-1.28	5.0	17.5 ± 0.8
	4.18-4.94	6.0	13.8 ± 0.7
	10.09-10.39	5.3	9.3 ± 0.7
	13.87-14.23	6.8	21.7 ± 0.7
	17.16-17.43	7.6	5.2 ± 0.4
HBF 10m	0.00-0.88	5.0	37.8 ± 1.1
	2.93-4.94	6.1	31.7 ± 0.9
	9.94-10.42	7.3	42.2 ± 0.9
	20.21-20.36	8.8	5.9 ± 0.4
	25.69-26.43	4.4	10.9 ± 0.8
RFF 0m	0.06-1.28	3.7	17.2 ± 1.2
	2.53-2.65	4.0	7.8 ± 0.9
	6.07-6.19	2.4	15.5 ± 1.4
	11.03-11.16	3.8	6.1 ± 0.9
	17.19-17.31	5.1	7.4 ± 0.7
	20.09-20.21	4.8	3.8 ± 0.9
EFF 0 m	1.43-1.83	5.0	24.4 ± 0.9
	4.48-4.88	4.8	33.2 ± 1.1
36-Chlorine			
Location	Depth (m)	$^{36}\text{Cl}/\text{Cl}$ ratio	
RFF 0m	5.91-6.43	$5.84\text{E-}13 \pm 1.30\text{E-}14$	
	9.75-9.88	$5.64\text{E-}13 \pm 1.30\text{E-}14$	
	13.78-14.30	$6.88\text{E-}13 \pm 3.40\text{E-}14$	
RFF 10m	5.03-5.30	$5.87\text{E-}13 \pm 1.40\text{E-}14$	
	10.24-10.61	$5.74\text{E-}13 \pm 1.30\text{E-}14$	
HBF 0 m	14.84-16.31	$5.68\text{E-}13 \pm 1.30\text{E-}14$	
HBF 50m	7.38-7.59	$4.72\text{E-}13 \pm 9.30\text{E-}15$	
RLB 0m	4.54-4.94	$7.50\text{E-}13 \pm 1.70\text{E-}14$	
EFF 92 0m	1.54-1.63	$4.37\text{E-}13 \pm 1.20\text{E-}14$	

Table 4. Tritium and $^{36}\text{Cl}/\text{Cl}$ ratios and stable isotopes in samples collected beneath and adjacent to fissures.

Stable isotopes			
Location	(depth in m)	$\delta^{18}\text{O}$	δD
RLB 0m	2.59-2.71	-7.9	-63
	5.46-7.16	-5.7	-50
	8.53-8.69	-6.8	-53
	11.55-11.80	-7.1	-54
	14.60-14.84	-7.5	-54
	20.51-20.63	-7.5	-55
RLB 50m	1.07-1.31	1.2	-36
	2.68-2.93	-2	-43
	4.88-5.12	-3.1	-46
	8.38-8.56	-3.9	-46
RFF 0m	3.47-3.6	-3.6	-44
	6.46-6.58	-4.8	-49
	9.51-9.63	-4.4	-49
	12.56-12.68	-5.4	-51
	18.81-18.93	-6	-56
	24.81-24.93	-6.9	-58